

# The Power of Radiocarbon in Biogeochemical Studies of the Marine Carbon Cycle: Insights from Studies of Dissolved and Particulate Organic Carbon (DOC and POC)

Ann P. McNichol\*<sup>†</sup> and Lihini I. Aluwihare<sup>‡</sup>

NOSAMS/Department of Marine Geochemistry and Geology, Woods Hole Oceanographic Institution, Woods Hole, Massachusetts 02543, and  
Geosciences Research Division, Scripps Institution of Oceanography, La Jolla, California 92093-0244

Received October 18, 2006

## Contents

1. Introduction	443
2. Radiocarbon	444
2.1. Basics	444
2.2. Terms and Definitions	445
2.3. Decay Counting	446
2.4. Accelerator Mass Spectrometry	446
2.5. Sample Preparation	447
3. Distribution of Radiocarbon in the Environment	447
3.1. Radiocarbon in the Ocean	449
3.2. General Biogeochemical Cycle of Radiocarbon	450
4. Dissolved Organic Carbon	450
4.1. Measurement/Isolation Techniques	450
4.2. Radiocarbon Measurements on Bulk DOC	452
4.3. Radiocarbon Measurements on Chemically Fractionated DOC	454
4.4. Radiocarbon Measurements on Size-Fractionated DOC	455
4.5. Radiocarbon Measurements on Compounds and Compound Classes	456
4.6. Sources of DOC Based on Radiocarbon Measurements	457
4.7. Summary	459
5. Particulate Organic Carbon	460
5.1. Collection/Isolation of POC	460
5.2. Radiocarbon Studies of POC	461
5.3. Summary	463
6. Summary and Future Directions	464
7. Acknowledgments	464
8. References	464

## 1. Introduction

In 1960, Willard F. Libby was awarded the Nobel Prize in Chemistry for developing the technique of radiocarbon ( $^{14}\text{C}$ ) dating. The importance of this technique for scientific studies of the natural environment has only grown as technological advances have improved the ability to measure this isotope. Carbon is one of the most important elements in the biosphere, and the ability to trace its path and residence

time in environmental reservoirs with a radioactive isotope enhances our ability to study biogeochemical cycles in the ocean.

This review focuses on radiocarbon in dissolved and particulate organic carbon (DOC and POC, respectively) in the open ocean. These marine reservoirs represent important sinks for atmospheric  $\text{CO}_2$ . For example, since sinking particles rapidly transfer material synthesized in the surface ocean, POC represents an important conduit for carbon transport from the surface (and, ultimately, the atmosphere) to the deep ocean or marine sediments, where it can be sequestered on long time scales. Dissolved organic carbon represents one of the largest exchangeable carbon pools on earth ( $\sim 650$  Gt C), containing as much carbon as is present in the atmosphere.<sup>1</sup> Therefore, small changes in the size of the DOC reservoir have the potential to significantly alter the concentration of  $\text{CO}_2$  in the atmosphere. Due to the important role these carbon reservoirs may play in the global carbon cycle, many studies have used radiocarbon in marine DOC and POC to investigate the cycling of carbon through these pools. Therefore, we choose to focus this review on biogeochemical insights into these reservoirs offered by radiocarbon studies. To our knowledge, there are no comprehensive reviews addressing radiocarbon-based studies of DOC and POC in the open ocean, and we will discuss results from the entire history of the field, from 1966 to the present. There is one published review on the carbon isotope composition of DOC by Bauer,<sup>2</sup> but the current review is more comprehensive in scope and covers some important advances in the field since the time of that review.

We begin this review by describing the basic theory and history behind making natural abundance radiocarbon measurements (section 2) and briefly outlining temporal and spatial variations in the distribution of  $^{14}\text{C}$  in various inorganic carbon reservoirs (section 3). Terminology in the radiocarbon field is very specific and sometimes confusing, and we feel it is important to summarize it here in some detail. Without the development of accelerator mass spectrometry (AMS), it would not have been possible to use radiocarbon to study the biogeochemical cycle of carbon in the oceans, and in section 2, we present a thorough review of AMS and where the technology is headed. Future advances in this field will continue to broaden the areas in which radiocarbon can help us understand the carbon cycle. Section 3 describes the distribution of radiocarbon in the environment, essentially describing the radiocarbon stage upon which biogeochemical processes occur. Our basic

<sup>†</sup> Woods Hole Oceanographic Institution.

<sup>‡</sup> Scripps Institution of Oceanography.



Ann P. McNichol is a Senior Research Specialist at the Woods Hole Oceanographic Institution (WHOI) in Woods Hole, MA. She received her B.S. in Chemistry from Trinity College in Hartford, CT, and her Ph.D. in Oceanography from the Massachusetts Institute of Technology (MIT)/Woods Hole Oceanographic Institution (WHOI) Joint Program in Oceanography (1986). She was a founding member of the National Ocean Sciences Accelerator Mass Spectrometry (NOSAMS) Facility at WHOI and was responsible for establishing the sample preparation laboratory. She focuses her research on developing methods to expand the use of  $^{14}\text{C}$  to study the ocean carbon cycle, studying the uptake of anthropogenic  $\text{CO}_2$  using  $^{13}\text{C}$  and  $^{14}\text{C}$ , and, recently, studying black carbon in the ocean and atmosphere.



Lihini Aluwihare is an Assistant Professor in the Geosciences Research Division of the Scripps Institution of Oceanography, a position she has held since 2001. She received her B.A. in Chemistry and Philosophy from Mount Holyoke College in 1993 and her Ph.D. in Oceanography from the Massachusetts Institute of Technology (MIT)/Woods Hole Oceanographic Institution (WHOI) Joint Program in Oceanography in 1999. Her research focuses on understanding the relationship between the various chemical environments of the ocean and the biological processes that take place within these environments. This research is carried out mainly in the context of studying the chemistry and biology of organic carbon and nitrogen. She and her research team draw on a variety of analytical tools from the fields of chemistry, biochemistry, isotope geochemistry, and molecular biology to study biological transformations of carbon and nitrogen in the marine environment.

knowledge of radiocarbon in the ocean and atmosphere has been catalogued well in the past and, recently, in much more detail. Given the residence time of the pools of carbon in the ocean, it is important to understand the current and past distribution of radiocarbon in the environment well. These discussions provide the background necessary to understand the extent of the limitations posed by analytical techniques and interpret the DOC (section 4) and POC (section 5) data in the context of their biogeochemistry.

Section 4 details radiocarbon studies of DOC, a chemically heterogeneous reservoir of carbon which is present in ocean

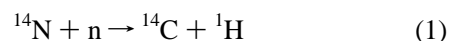
waters at concentrations between 40 and 100  $\mu\text{M C}$ .<sup>1</sup> The ability to place limits on sources and residence times of the complex DOC reservoir with the use of radiocarbon is adding greatly to our understanding of it. The discussion presented in section 4 shows that the DOC reservoir in the ocean consists of a mixture of components with radiocarbon signatures ( $\text{DO}^{14}\text{C}$ ) ranging from values similar to that of dissolved inorganic carbon (DIC) in surface waters<sup>3</sup> to values as depleted as  $-800\%$ .<sup>4</sup> The average  $\text{DO}^{14}\text{C}$  values in surface waters are between  $-150\%$  and  $-400\%$ , and the average  $\text{DO}^{14}\text{C}$  value of the oldest water mass (North Pacific Deep Water) is  $-540\%$ .<sup>5</sup> Based on comparisons to the radiocarbon content of DIC ( $\text{DI}^{14}\text{C}$ ), it is clear that the average residence time of marine DOC is several times longer than the time required for one ocean-mixing cycle, suggesting that a refractory DOC component exists well mixed throughout the water column (see, e.g., Williams and Druffel<sup>6</sup>). Despite the low radiocarbon values of the surface DOC reservoir, mass balance calculations indicate that DOC derived from recent photosynthesis accumulates in this reservoir.<sup>5,7</sup> However, it was not until the first compound-specific radiocarbon measurements were made that conclusive evidence in support of this hypothesis was presented.<sup>3,8</sup> These latter studies also provide evidence to suggest that while the bulk DOC reservoir may be distributed to deep ocean basins via water mass advection (similar to DIC), some components of DOC are added to the deep ocean during dissolution of rapidly sinking particles.<sup>3</sup> This “fresh” DOC may be vital in sustaining the communities of heterotrophic bacteria that have been identified in meso- and bathypelagic environments.<sup>9,10</sup>

Section 5 reviews radiocarbon studies of particulate organic carbon (POC). Radiocarbon studies of both the suspended ( $\text{POC}_{\text{susp}}$ ) and sinking ( $\text{POC}_{\text{sink}}$ ) pools demonstrate that POC cycles much more rapidly than DOC, as it contains bomb produced  $^{14}\text{C}$  (see section 3) throughout the water column. The presence of bomb- $^{14}\text{C}$  in POC reflects its source from the recent (post-1960, see section 3) synthesis of material from DIC in surface waters and the subsequent rapid transport to subsurface depths. Decreases in the radiocarbon content of  $\text{POC}_{\text{susp}}$  ( $\text{PO}^{14}\text{C}_{\text{susp}}$ ) with depth are seen in all oceans and are thought to result from the absorption of  $^{14}\text{C}$ -depleted DOC at depth. However, close to ocean margins, horizontal export of  $^{14}\text{C}$ -depleted POC could also contribute to the observed decreased in  $\text{PO}^{14}\text{C}_{\text{susp}}$ .

## 2. Radiocarbon

### 2.1. Basics

Radiocarbon,  $^{14}\text{C}$ , is the most abundant radioactive isotope of carbon and is generated in the upper stratosphere and lower troposphere by the reaction of cosmic rays with nitrogen in the reaction<sup>11</sup>



The  $^{14}\text{C}$  formed in eq 1 is rapidly oxidized to  $\text{CO}_2$  and becomes a part of the global carbon cycle. The stable isotopes,  $^{12}\text{C}$  and  $^{13}\text{C}$ , are the most abundant isotopes of carbon; the approximate natural abundance of  $^{14}\text{C}$  is 1 atom per every  $10^{12}$ – $10^{13}$  atoms of C. Radiocarbon decays with a half-life of 5730 years<sup>12</sup> and is ideal for the study of biogeochemical processes that occurred over the past 50,000 years. Suggestions that the half-life may be significantly in

error<sup>13</sup> do not appear to be substantiated by recent data (Roberts, M. L.; Southon, J. R. Personal communication). Studying radiocarbon requires the adoption of a new language, and it is important to understand the nomenclature and conventions before reviewing our current state of knowledge.

## 2.2. Terms and Definitions

Radiocarbon is measured as either a specific activity (A) or an isotopic ratio (<sup>14</sup>R), where <sup>14</sup>R is the ratio of <sup>14</sup>C to either <sup>13</sup>C or <sup>12</sup>C, i.e., <sup>14</sup>R = <sup>14</sup>C/<sup>13</sup>C or <sup>14</sup>C/<sup>12</sup>C.<sup>14–16</sup> To use radiocarbon for dating purposes, a starting point for the time line had to be established, i.e., a theoretical time zero. The year 1950 was chosen as the base year for all radiocarbon measurements and is considered modern, or present. Although there is no *a priori* reason for choosing 1950 as time zero, it is convenient because of the history of radiocarbon in the atmosphere. Samples more recent than 1950 are likely to be influenced by bomb-produced <sup>14</sup>C, complicating the use of radiocarbon as a dating and source identification tool. Typically, the <sup>14</sup>C content of a sample is expressed as a deviation from a known standard (whose <sup>14</sup>C content represents modern/time zero). To avoid the influence of atmospheric radiocarbon fluctuations from burning of fossil fuel since the Industrial Revolution or nuclear weapons testing during the 1950s and 60s, the <sup>14</sup>C activity of “1890 wood” corrected to the activity it would have in 1950 was chosen as the absolute standard. This standard has since been replaced by NIST SRM 4990B (oxalic acid I, HOxI) and, subsequently, SRM 4990C (oxalic acid II, HOxII).<sup>17</sup> By definition, modern (A<sub>m</sub>, R<sub>m</sub>) is 95% of the activity or ratio of HOxI.<sup>17</sup> All sample measurements are reported relative to modern. For the remainder of this discussion, we will refer to isotopic ratios (<sup>14</sup>R) rather than activities (A), as this is the quantity measured most frequently. Because specific activity is proportional to the ratio of <sup>14</sup>C to the total carbon in a sample, A can be substituted for R in eqs 2–6 listed below.

Radiocarbon is subject to isotopic fractionation during natural processes just as <sup>13</sup>C is (e.g., when atmospheric CO<sub>2</sub> is incorporated into organic matter during photosynthesis), and the <sup>14</sup>C isotopic ratios measured in a sample will reflect this fractionation as well as radioactive decay. Every <sup>14</sup>R is corrected to reflect the value it would have if its δ<sup>13</sup>C were –25‰; that is, it is normalized to –25‰, the δ<sup>13</sup>C value of the theoretical “1890 wood” standard. If this is not done, <sup>14</sup>R would reflect both aging and isotopic fractionation. Normalizing the sample allows the user to compare <sup>14</sup>C differences between carbon reservoirs due primarily to <sup>14</sup>C decay. To normalize the sample, fractionation between <sup>14</sup>C and <sup>12</sup>C is assumed to be approximately twice that between <sup>13</sup>C and <sup>12</sup>C.<sup>15,16</sup> Finally, for historical purposes, HOxI is normalized to a value of –19.0‰, its most likely actual value. The fractionation correction differs depending on whether <sup>14</sup>C/<sup>12</sup>C or <sup>14</sup>C/<sup>13</sup>C is measured.<sup>18</sup> These corrections are listed below.

For labs measuring <sup>14</sup>C/<sup>12</sup>C

$$R_{sn} = R_s \left[ \frac{1 + 0.001 * (-25)}{1 + 0.001 * \delta^{13}C_s} \right]^2 \quad (2)$$

where

$$\delta^{13}C = \left[ \frac{^{13}R_{\text{sample}}}{^{13}R_{\text{standard}}} - 1 \right] \times 1000$$

For labs measuring <sup>14</sup>C/<sup>13</sup>C

$$R_{sn} = R_s \left[ \frac{1 + 0.001 * (-25)}{1 + 0.001 * \delta^{13}C_s} \right] \quad (3)$$

where s refers to sample and n indicates R has been normalized.

Radiocarbon values are usually reported as fraction modern (fm), percent modern (pM), radiocarbon age (<sup>14</sup>C yr), or Δ<sup>14</sup>C. These terms are used as defined in Stuiver and Polach 1977<sup>14</sup> with the additions and amendments described in Stuiver,<sup>19,20</sup> Mook,<sup>21</sup> and Long<sup>22</sup> and as summarized here. Based on these definitions, we can express the terms used to report radiocarbon values as follows:

$$\text{fm} = 0.01(\text{pM}) = R_{sn}/R_m \quad (4)$$

$$^{14}\text{C yr} = -8033 \ln(\text{fm}) \quad (5)$$

where 8033 year is based on the Libby half-life of <sup>14</sup>C

$$\Delta^{14}\text{C} = 1000[\text{fm} \exp^{-\lambda(y-1950)} - 1] \quad (6)$$

where y is the year of sample collection or growth year of the sample and λ = 1.201 × 10<sup>–4</sup> is the decay constant for <sup>14</sup>C based on the real half-life.<sup>14</sup>

The relationship of each of these terms is shown in Figure 1. fm and pM report the fractional amount of <sup>14</sup>C in a sample

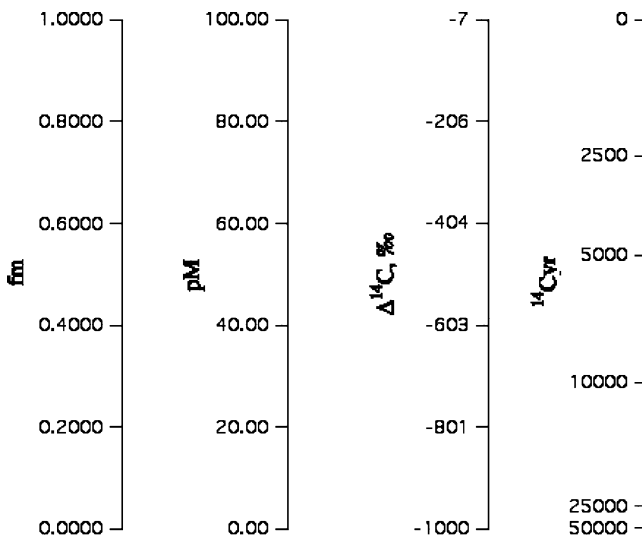


**Figure 1.** The relationship of four radiocarbon scales commonly used in ocean biogeochemistry. The Δ<sup>14</sup>C scale is calibrated for a sample collected in 2006. Definitions of the terms appear in the text.

relative to that found in the standard. A radiocarbon age, <sup>14</sup>C yr, is not a calendar or chronological age and must be calibrated. In oceanography and carbon cycle studies, the concept of age is particularly problematic. The variety of carbon sources to the ocean and the mixing and movement of different water masses result in carbon with a variety of ages being used in all parts of the carbon cycle. Because of this, Δ<sup>14</sup>C, which normalizes the radiocarbon content of a sample to the same δ<sup>13</sup>C (–25‰) and time point (1950), is

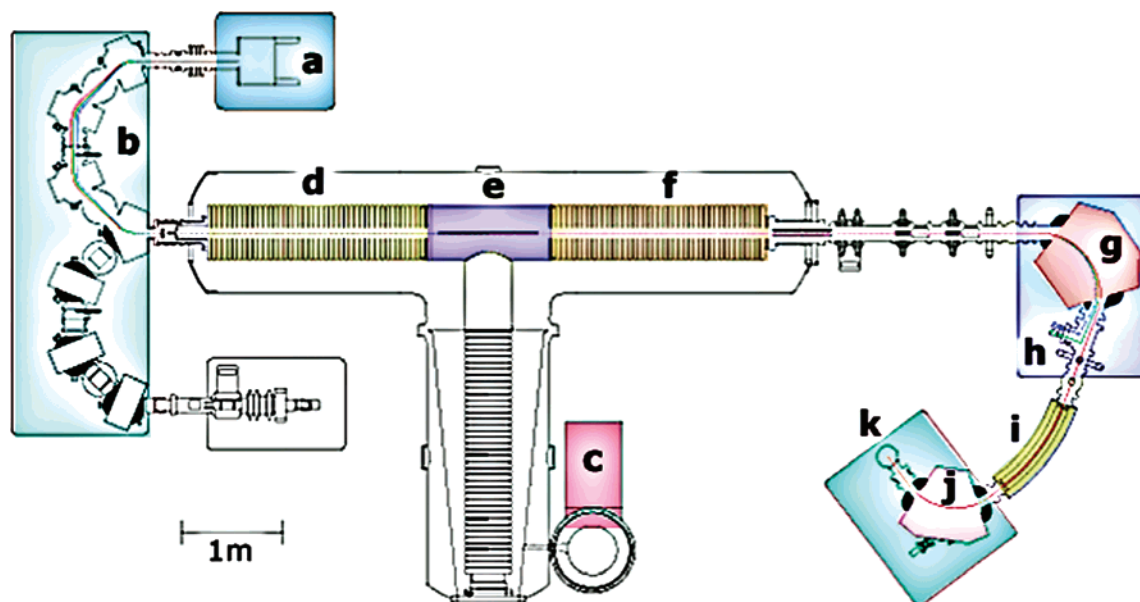


**Figure 2.** Schematic of a 3 MV AMS in operation at the National Ocean Sciences AMS Facility (NOSAMS). Detailed descriptions of the (a) ion source, (b) recombinator region, (c) power supply, (d and f) accelerator tubes, (e) stripper canal, (g and j) analyzer magnets, (h) Faraday cups, (i) electrostatic deflector, and (k)  $^{14}\text{C}$  detector appear in the text.

a useful parameter. Further, it is a linear quantity and can be used in mass balances. In this review, when we report a radiocarbon value and its associated error, we refer to the 1 sigma error unless otherwise stated.

### 2.3. Decay Counting

Prior to the 1980s, all radiocarbon measurements were made by counting the radioactive decay products of  $^{14}\text{C}$ , either with gas proportional or liquid scintillation counting. Comprehensive reviews of these techniques exist (e.g., Polach<sup>23</sup>), and they will not be covered in detail here. Decay counting techniques severely limited the scope of radiocarbon studies because of the size of the sample required (grams of carbon) and the time required to collect precise results (days to weeks). The heroic efforts of early researchers to collect and measure radiocarbon samples in the ocean using these techniques provided information that started to reveal the complexity of the carbon cycle and demonstrated the potential insight that could be gained if detection limits for  $^{14}\text{C}$  could be improved. Although research is still conducted using counting methods, accelerator mass spectrometry (AMS), a much more sensitive technique, is eclipsing these studies with its tremendous advantages.

### 2.4. Accelerator Mass Spectrometry

In the 1970s and 1980s, AMS was developed to measure  $^{14}\text{C}$  and other rare isotopes.<sup>24</sup> The marriage of middle energy physics with mass spectrometry allowed analysts to count the number of  $^{14}\text{C}$  atoms in a sample rather than wait for a decay event to occur. This reduced the amount of time required to count a sample precisely to less than an hour and the amount of sample required to milligram quantities. This revolutionary development opened the world of radiocarbon to many more researchers. In its infancy, it was presumed that AMS could never achieve the same level of precision as decay counting. This has proven untrue, and laboratories routinely achieve precisions of 3–7‰ on modern samples of a standard size (>500  $\mu\text{g C}$ ). With abundant sample, a high-energy ion source, and an increased number

of standards during analysis, even higher precision can be obtained (2–3‰).<sup>25</sup> For most biogeochemical studies, however, standard precision levels are more than adequate. A brief description of AMS as it applies to the study of radiocarbon follows.

A number of different accelerators are in use around the world for the analysis of radiocarbon, and we will not describe all the variations that exist. An example is shown in Figure 2, and the lettered sections of the accelerator shown in the figure are described in detail in the following text (marked in bold here). Currently, most radiocarbon laboratories prepare targets for AMS by converting the carbon in a sample to filamentous carbon generated on a metal catalyst. The solid carbon and metal sample, commonly referred to as a graphite target, is compressed into a target holder and transferred to the ion source (a). Here, a cesium (Cs) ion beam directed at the sample generates negative ions from the carbon in the target. Although the production of negative ions is inefficient, ranging from 3 to 10% depending on the ion source, this is an important step. Nitrogen, which has a mass of 14 and could overwhelm the detection of  $^{14}\text{C}$ , does not form a negative isobar. Thus, it is not converted to an ion and is effectively removed from the system. The extracted beam is passed through a magnetic region, either a recombinator (b) or a bouncer system. In both systems, the beam is passed through a magnet region to isolate masses 12, 13, and 14 from higher and lower mass impurities. In the recombinator system, the three masses are then “recombined” and introduced to the accelerator, while in the bouncer system, each mass is introduced to the accelerator sequentially. Sequential systems measure masses 14, 13, and, sometimes, 12. The singly charged beam(s) are passed through an accelerating potential (d) of 0.5–10 MV depending on the accelerator. These ions are stripped of electrons in the stripper canal (e) to form positively charged ions that are then passed through a second accelerating potential (f). The stripping process also destroys most of the molecular ions, such as  $^{13}\text{CH}^-$  and  $^{12}\text{CH}_2^-$ , which have masses that may interfere with the detection of  $^{14}\text{C}$ . The charge state of the positive ions depends on the accelerator that is being

used and most commonly ranges from +1 to +4. At this stage, the beam is passed through an analyzing magnet (g) and  $^{12}\text{C}$  and/or  $^{13}\text{C}$  ion currents are measured with a Faraday cup(s) (h). The  $^{14}\text{C}$  beam is passed through an electrostatic deflector (i) that discriminates particles based on their charge/mass ratio. Radiocarbon atoms can be counted using different detectors, the most common of which are gas ionization or solid-state detectors. The energy imparted by the accelerator facilitates the measurement because the natural abundance of  $^{14}\text{C}$  is so low relative to those of  $^{12}\text{C}$  and  $^{13}\text{C}$ . The molecular fragments that have masses almost identical to that of  $^{14}\text{C}$  are more efficiently destroyed by the high energy produced in an accelerator.

Current research efforts in AMS are aimed at reducing the operating energy of the accelerator and developing a gas ion source so that  $\text{CO}_2$  gas can be directly introduced into the accelerator.<sup>26</sup> Lower energy machines are smaller, are less costly to purchase and maintain, and will make radiocarbon measurements more accessible. At present the lowest energy machines in use are 500 kV, but studies are investigating the utility of using energies as low as 200 kV.<sup>26</sup> Evidence indicates that the 500 kV instruments can provide the same range of precision and background as larger machines. The ultimate role of gas ion sources in the natural radiocarbon field is evolving at present. Simply converting a sample to  $\text{CO}_2$  rather than reducing it to carbon and pressing the sample into a cartridge removes a number of steps where carbon may be added as a process blank and reduces the time required to process a sample. Additionally, the gas ion sources open the possibility of directly injecting samples from separation devices such as gas or liquid chromatographs and laser ablation systems. Early gas sources modified conventional sputter sources to accept the introduction of  $\text{CO}_2$  and were limited by the observed background and the presence of memory effects.<sup>27</sup> The theoretical limits for the gas ion source developed at Oxford indicate the superiority of their source for very small samples ( $\leq 1\text{--}2\ \mu\text{g C}$ ),<sup>28</sup> but in practice, the most precise results and the best backgrounds on the smallest samples are measured on solid carbon targets.<sup>29,30</sup> Newer studies are developing ion sources specifically designed to handle gases and show promise for natural-abundance samples. Early results from a continuous-flow AMS system indicate the possibility of obtaining 10% precision on half-modern samples containing as little as 2.5  $\mu\text{g C}$ .<sup>31</sup>

## 2.5. Sample Preparation

The adoption of AMS revolutionized the radiocarbon community by reducing the size of the sample required from grams to milligrams. Successful work at these levels has led researchers to clamor for even smaller sample sizes to be run, and the AMS community has been able to reduce the size requirement to micrograms.<sup>32,29</sup> This development is critical to the field of ocean biogeochemistry, since most studies are carbon-limited. However, the limitations imposed by the analysis of smaller samples must be recognized. Pearson et al.<sup>32</sup> demonstrate the successful analysis of samples containing as little as 20  $\mu\text{g C}$  with a precision of 15–25%. dos Santos<sup>33</sup> demonstrated the capability to measure samples as small as 2  $\mu\text{g}$  on an accelerator with a precision of approximately 30%. This is a tremendous development that Shah and Pearson<sup>30</sup> demonstrate has put the capability of the accelerator ahead of the ability of organic geochemists to isolate clean samples. Any handling, whether

chemical or physical, can add carbon to a sample (referred to here as a process blank), and this carbon may or may not contain radiocarbon. Specialized sample preparations, e.g., solvent extraction and chromatographic isolation, will have process blanks that depend on the specific preparation, and these must be determined for each step and/or method. Determining the age of the carbon added is more problematic. In some cases, the quantity of sample carbon is too low to allow direct measurement of an individual sample and researchers resort to standard addition techniques or pooling of samples. In general, process blanks contain  $^{14}\text{C}$  signatures that indicate the contaminating carbon is a mixture derived from modern and dead sources. When it is not possible to measure the fm value of the process blank, it is possible to calculate a range of expected fm values for a sample by assuming the process blank is either completely  $^{14}\text{C}$ -free (fm = 0) or totally modern (fm = 1).<sup>34</sup>

A comprehensive study of the sources, magnitudes, and fm values of process blanks introduced during the isolation of lipids from marine samples indicates that each step adds measurable amounts of carbon with fm values that vary from dead to modern.<sup>30,35</sup> The amounts vary from very small, 0.03  $\mu\text{g mL}$  from an HPLC, to somewhat large, 1  $\mu\text{g C}$  from closed-tube combustion. The latter value is in the range measured by others, approximately 0.5–1.5  $\mu\text{g C}$ .<sup>32,34,36–38</sup> Currie et al.<sup>36</sup> demonstrated that the combustion blank could be reduced to 0.16  $\mu\text{g C}$  using the cleanest chemical techniques available. In addition, Shah and Pearson<sup>30</sup> show that, until the magnitude of the error in the determination of the C amount and the  $^{14}\text{C}$  content of process blanks can be reduced, samples containing less than 5  $\mu\text{g C}$  can only be measured to precisions of hundreds of per mille units. Isotope dilution is another path to analyzing the smallest samples.<sup>32,36</sup> Currie et al.<sup>36</sup> increased the amount of carbon in small samples to 25  $\mu\text{g C}$  by adding  $\text{CO}_2$  from a source whose  $^{14}\text{C}$  content was well-known. We refer to this technique here as dilution. The dilution ratio, i.e., total mass/sample mass, was measured accurately and precisely using a small quadrupole mass spectrometer. The study's results indicate that this technique limits researchers to analyzing samples containing as little as 3  $\mu\text{g C}$  in studies assessing the presence or absence of  $^{14}\text{C}$ .<sup>17,36</sup>

## 3. Distribution of Radiocarbon in the Environment

Radiocarbon is a useful, but complex, tool for studying biogeochemical cycling in the oceans. Radiocarbon formed in the atmosphere is rapidly converted to  $\text{CO}_2$  and enters the biogeochemical cycle through physical (e.g., dissolution in seawater) and biological (e.g., photosynthesis) processes (Figure 3).  $\Delta^{14}\text{C}$  values of autotrophs, e.g., photosynthetic organisms, reflect the  $\Delta^{14}\text{C}$  value of the inorganic carbon source. Therefore, terrestrial and marine plants have distinct  $\Delta^{14}\text{C}$  signatures reflecting the difference in  $\Delta^{14}\text{C}$  of atmospheric  $\text{CO}_2$  versus DIC in the surface ocean. Heterotrophic consumers acquire carbon with essentially the same ratio as the source of their sustenance; that is, you are what you eat. While living, organisms maintain a  $^{14}\text{C}$  content that reflects their source carbon. Upon death, carbon exchange between the organism and the environment ceases and starts the radiocarbon clock.

The use of radiocarbon as a chronological tool directly requires that the production of radiocarbon in the atmosphere be constant over time. However, since the flux of cosmic

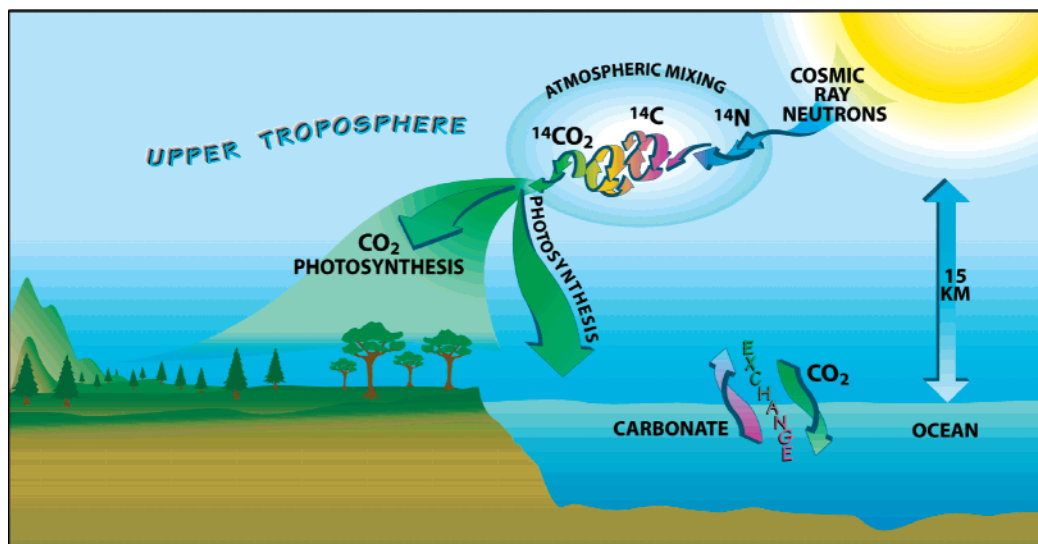


**Figure 3.** Illustration of the natural  $^{14}\text{C}$  cycle (Reprinted with permission from Jayne Doucette, Woods Hole Oceanographic Institution).

rays that produce radiocarbon varies over time, the  $^{14}\text{C}$  content of the atmosphere fluctuates. Figure 4 shows the

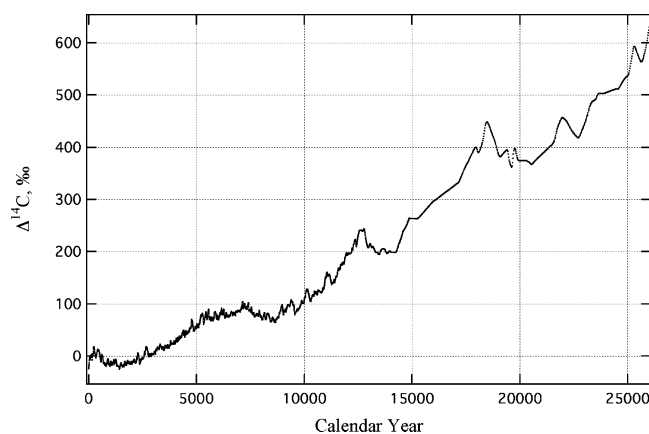


**Figure 4.**  $\Delta^{14}\text{C}$  in the atmosphere as a function of calendar year; data obtained from INTCAL04 (references in text).

variation in atmospheric  $\Delta^{14}\text{C}$  over the past 26,000 years.<sup>39</sup> Records of the atmospheric history of radiocarbon are stored in tree rings, and these have been used to calibrate the radiocarbon time scale.<sup>40</sup> Presently, the tree ring history extends back to 12,400 year, and other records are being used to extend the calibration further in time. Records preserved in corals, speleothems, varved sediments, and terrestrial cores have extended the record back to 26,000 year and are extending it to 40,000–50,000 calendar years.<sup>13,41,42</sup>

Anthropogenic disruptions in the atmospheric radiocarbon concentration started occurring in the 1800s. The use of fossil fuel as an energy source adds  $\text{CO}_2$  with no  $^{14}\text{C}$ , i.e., radiocarbon-dead, to the atmosphere and has led to an observable temporal decrease in  $\Delta^{14}\text{C}$ , commonly referred to as the Suess Effect.<sup>43</sup> From 1890 to 1950,  $\Delta^{14}\text{C}$  observed in tree rings from the North American Pacific coast decreased about 20%.<sup>44</sup> It was estimated that about 17% of this decrease was due to the addition of  $\text{CO}_2$  from fossil fuel burning. A large  $^{14}\text{C}$  spike was introduced into the atmosphere in the 1950s and 1960s as a result of above-ground nuclear weapons testing. This addition almost doubled the atmospheric inventory and slowly entered the surface ocean DIC reservoir through air–sea gas exchange. Figure 5 summarizes the atmospheric and surface ocean marine

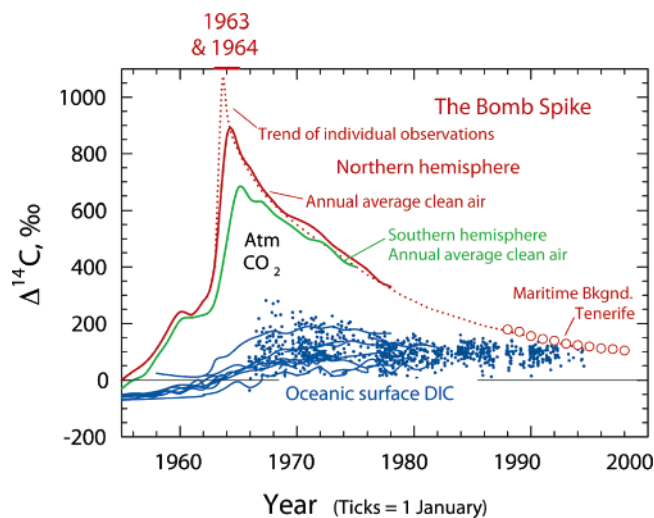


**Figure 5.** Radiocarbon levels ( $\Delta^{14}\text{C}$ ) in atmospheric  $\text{CO}_2$  and surface ocean  $\text{DI}^{14}\text{C}$  since 1955. The red dashes and circles represent individual measurements; red and green lines show annual average clean air; blue dots represent measurements of surface  $\text{DI}^{14}\text{C}$ ; blue lines are ocean surface data reconstructed from coral measurements. References are cited in the text.

observations that have been made in recent times. Data for this figure were compiled from individual observations,<sup>45–47</sup> an annual average for clean air calculated by Tans,<sup>48</sup> surface water measurements collected in the Atlantic, Pacific, and Indian Oceans between 1965 and 1994,<sup>49</sup> and surface values derived from coral records<sup>50,51</sup> and accessible at <http://www.ncdc.noaa.gov/paleo/coral/coral14c.html>. The atmospheric spike in  $\Delta^{14}\text{C}$  of  $\text{CO}_2$  is clear and large. The appearance of the spike in surface ocean DIC is dampened and delayed due to the ocean reservoir size and to the relatively long time (approximately 10 years) required to reach isotopic equilibrium between the atmosphere and surface ocean. The hemispheric difference in the atmosphere arises because most of the weapons testing took place in the northern hemisphere and interhemispheric air mixing occurs on the time scale of 1 year. The large scatter observed in surface ocean measurements primarily reflects the complex circulation of the oceans, and not variability seen at individual locations. Although the introduction of this spike has complicated the use of radiocarbon as a strict dating tool,

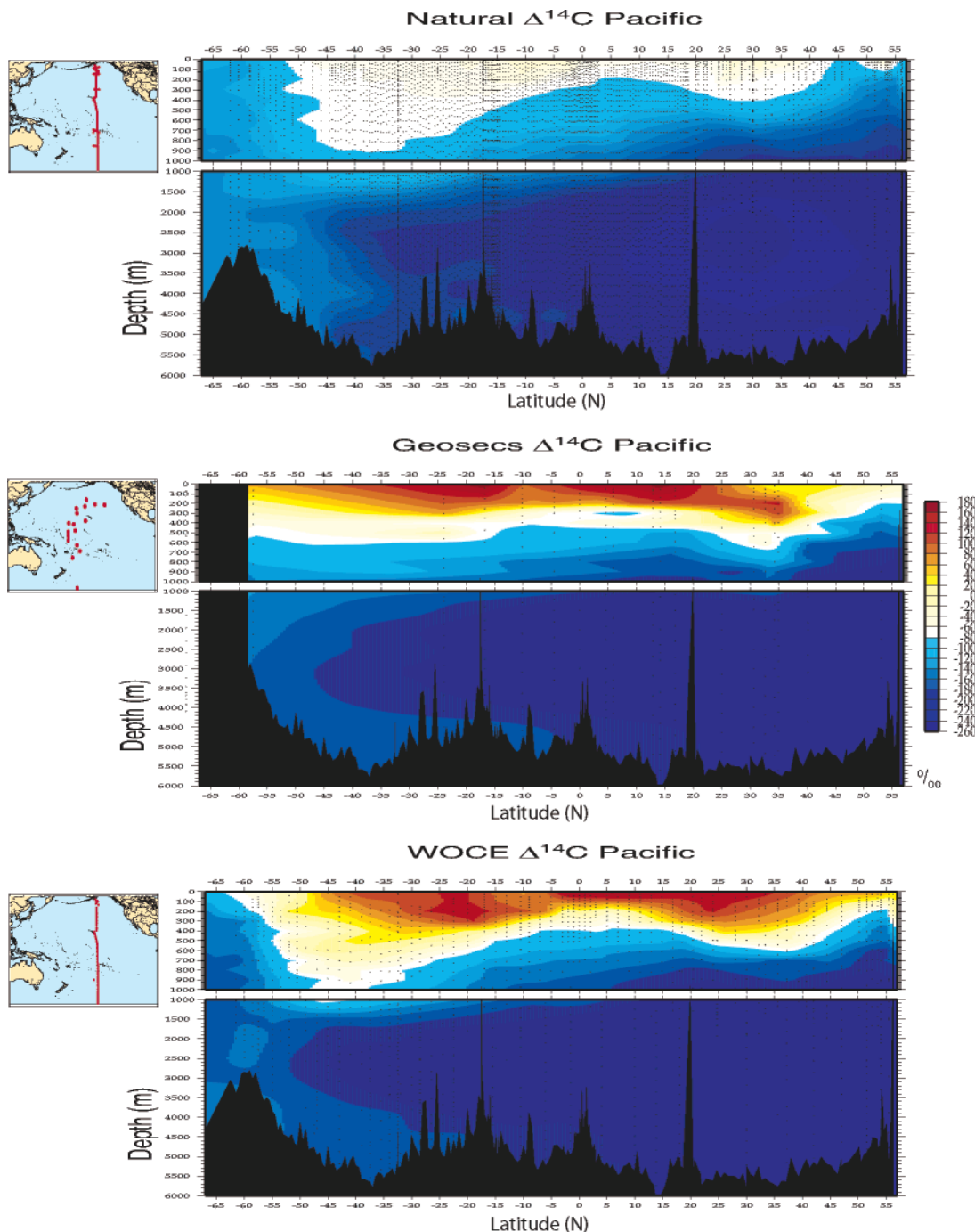


**Figure 6.** Vertical distribution of  $\text{DI}^{14}\text{C}$  in the Pacific Ocean (a) prior to anthropogenic influence along  $150^\circ\text{W}$ , (b) in the 1970s in the western section from GEOSECS, and (c) in the 1990s along  $150^\circ\text{W}$ .

it has also acted as a useful natural experiment making it possible to trace the spike throughout natural carbon reservoirs that interact on time scales less than 50 years (i.e., time scales shorter than the time scale over which measurable decay-induced changes in  $\Delta^{14}\text{C}$  occur).

### 3.1. Radiocarbon in the Ocean

Radiocarbon enters the ocean through many paths, but primarily through the equilibration of seawater DIC with atmospheric  $\text{CO}_2$ . Circulation of the ocean redistributes DIC, and the  $^{14}\text{C}$  content of any parcel of water is related to both its ventilation history, i.e., the amount of time it has been isolated from exchange with the atmosphere, and its source water composition. Ocean surveys conducted in the 1970s

(the GEOSECS program<sup>52–54</sup>), the 1980s (TTO<sup>55</sup> and SAVE<sup>56,57</sup>), and the 1990s (the WOCE program<sup>58</sup>) provide snapshots of the  $\text{DI}^{14}\text{C}$  distribution in the world's oceans. Figure 6 shows some examples of  $\text{DI}^{14}\text{C}$  patterns in the Pacific Ocean. In this figure, the top panel shows the distribution of  $\text{DI}^{14}\text{C}$  prior to fossil fuel combustion and nuclear weapons testing, i.e., preindustrial, pre-nuclear (PIP-N). The PIP-N  $\text{DI}^{14}\text{C}$  distribution is calculated from  $\Delta^{14}\text{C}$  observations made in 1991/2 during the WOCE program and using the relationship between  $\Delta^{14}\text{C}$  and potential alkalinity (PALK) observed by Rubin and Key<sup>59</sup> to correct for the uptake of  $^{14}\text{C}$  introduced by anthropogenic activities. The second two panels show the distributions of  $\text{DI}^{14}\text{C}$  measured during the 1970s GEOSECS program and the 1990s WOCE

program. Distinct patterns of high and low values of  $\text{DI}^{14}\text{C}$  are evident and arise from the circulation patterns of the ocean. The uptake of bomb radiocarbon is most evident in the gyres ( $10^\circ\text{S}$ – $40^\circ\text{S}$  and  $5^\circ\text{S}$ – $40^\circ\text{N}$ ) where there is more time for equilibration with the atmosphere. The  $^{14}\text{C}$  depletion resulting from radioactive decay in North Pacific Deep Water is seen in each figure; this is the oldest water mass in the ocean, and its  $\Delta^{14}\text{C}$  values correspond to over 2000  $^{14}\text{C}$  yr. Different but similarly distinct patterns in  $\text{DI}^{14}\text{C}$  are present in all ocean basins. General patterns that are evident in other regions are the transfer of  $^{14}\text{C}$  to greater depths in regions of deep water formation and the transfer of  $^{14}\text{C}$ -depleted waters to the surface through upwelling. Descriptions and data can be found in the literature (references above) and on Web sites (e.g., [http://www-pord.ucsd.edu/whp\\_atlas/](http://www-pord.ucsd.edu/whp_atlas/); <http://cdiac3.ornl.gov/waves/>). Based on Figure 6 (last panel), it is clear that bomb  $^{14}\text{C}$  is present throughout the surface ocean DIC reservoir, but below approximately 2000 m in the Pacific, there is little evidence of bomb  $^{14}\text{C}$ . If other reservoirs of carbon in the deep ocean and sediments contain bomb  $^{14}\text{C}$ , it must be delivered via sinking inorganic and organic particles originating in the surface ocean.

Detailed time histories of  $\text{DI}^{14}\text{C}$  in the surface ocean are recorded in ocean corals and long-lived mollusks. These histories augment the global snapshots obtained during the water sampling programs and provide a way to directly measure prebomb  $\text{DI}^{14}\text{C}$  in the ocean. Marine prebomb  $\text{DI}^{14}\text{C}$  values are required to accurately interpret the cycling of carbon through the various reservoirs. For example, estimating the time scale on which deep water masses circulate requires both the vertical  $\Delta^{14}\text{C}$  distributions shown in Figure 6 (for example) and a measure of prebomb  $\text{DI}^{14}\text{C}$  (i.e., the  $\Delta^{14}\text{C}$  signature of these water masses at the time of last contact with the atmosphere). In the western equatorial Pacific Ocean, a high-resolution coral record collected near Nauru Island<sup>60</sup> (Figure 7) demonstrates the intrusion of the

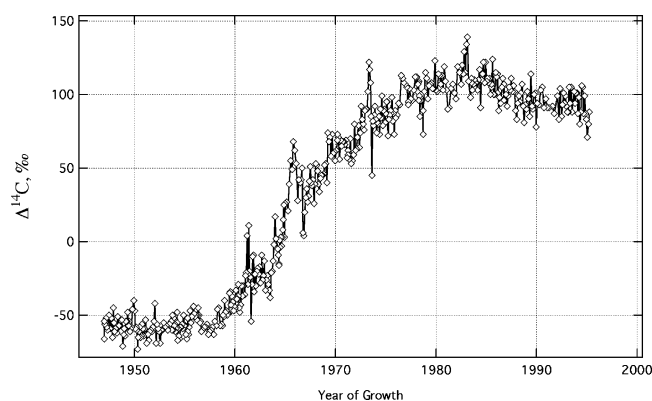


**Figure 7.** High-resolution record of  $\Delta^{14}\text{C}$  in coral collected at Nauru Island in the western equatorial Pacific (references in text).

atmospheric bomb signal into the surface ocean and also points out the impact of regional ocean processes. Strong deviations from the general trend are correlated with El Niño–Southern Oscillation (ENSO) events, and the magnitude and direction of the deviation can be explained as ENSO-driven changes in the amount of upwelling at this site.<sup>61</sup> Records exist for corals collected in other Pacific locations,<sup>50,51</sup> the Atlantic,<sup>62</sup> and the Indian<sup>63–65</sup> Ocean. The  $\text{DI}^{14}\text{C}$  history of regions where corals do not grow has been documented using other strategies. In the North Atlantic, for example, records have been obtained from Arctica Islandica,

a long-lived mollusk,<sup>66</sup> and in the North Pacific, archived fish scales may provide a means of obtaining these records. In the ocean, the radiocarbon content of organisms and their organic molecules will depend heavily on the region and depth of the ocean where they were produced and, more recently, when they were produced.

### 3.2. General Biogeochemical Cycle of Radiocarbon

In addition to equilibration of the surface ocean with the atmosphere, radiocarbon enters the marine environment through other pathways. Radiocarbon signatures of bulk pools of organic carbon in the ocean and the pathways by which  $^{14}\text{C}$  can be added to the ocean are summarized in Figure 8. Allochthonous carbon, with its burden of  $^{14}\text{C}$ , enters from the terrestrial environment through river runoff, erosion, and atmospheric deposition from dust. This material can consist of fresh and pre-aged carbon from a variety of different sources with a full spectrum of chemical reactivity. Carbon can enter the water column from the subsurface as well, e.g., diffusion from sediment pore water, seeps from petroleum and gas reservoirs, hydrothermal vents, and resuspension of surface sediments. Biogeochemical processes in the ocean repackage and redistribute inorganic carbon and impact the observed radiocarbon distributions. Auto- and heterotrophy in the upper water column produce organic matter that can become a source of DIC, DOC, and POC throughout the water column. The majority of organic carbon within the ocean is derived from photosynthesis in surface waters, thus  $\text{DI}^{14}\text{C}$  in surface waters is expected to have the greatest influence on the  $^{14}\text{C}$  content of organic matter throughout the water column. As will be clear in the following sections (and as shown in Figure 8), the  $\Delta^{14}\text{C}$  of some fractions of marine organic carbon deviates from this expectation. For example, the presence of DOC with depleted  $\Delta^{14}\text{C}$  values despite delivery of fresh organic matter to the deep water column and surface sediments remains a mystery that is currently the subject of much study. Also, chemoautotrophic synthesis of organic matter in the deep ocean can produce some new organic matter with depleted radiocarbon signatures.

In general, carbon from a variety of sources has the potential to become actively involved in marine biogeochemical cycles. Distinct radiocarbon signatures of the many pools lead to the power of this tracer in studies of carbon cycling, yet the overlapping signatures of many of the reservoirs lead to great complexity, making it difficult to delineate the exact interactions between reservoirs and assign unique processes that contribute to the observed signal. It is usually upon this complex stage that biogeochemical processes take place. The following discussion will provide examples of both the strength and challenges associated with using this tracer while highlighting the unique insights into marine carbon biogeochemistry that it provides.

## 4. Dissolved Organic Carbon

### 4.1. Measurement/Isolation Techniques

Marine DOC is a complex pool of carbon and its collection, isolation, and preparation for radiocarbon measurement require careful consideration and definition in order to provide meaningful results for the oceanographic community. As shown in Figure 9, DOC is not a discrete and



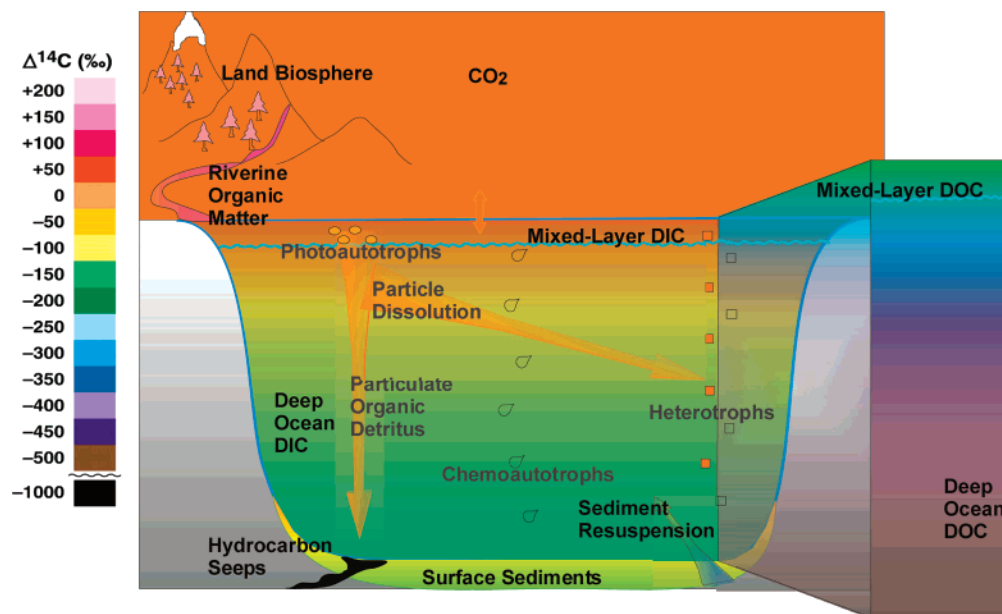


**Figure 8.**  $\Delta^{14}\text{C}$  values of inorganic and organic carbon reservoirs related to  $\text{DO}^{14}\text{C}$ . Adapted with permission from Pearson, A., Biogeochemical Application of Compound-Specific Radiocarbon Analysis. Ph.D. Thesis, MIT/WHOI: 2000; 00-01. Copyright 2000 A. Pearson.

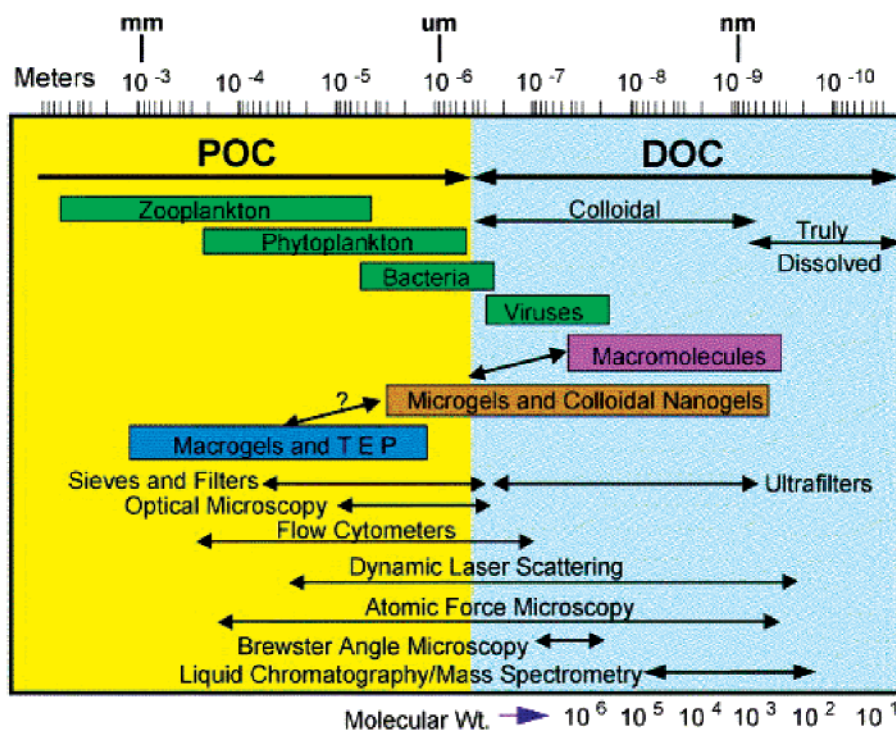


**Figure 9.** Definition of size distinctions for marine organic matter. Reprinted from ref 102, Copyright 2004, with permission from Elsevier.

easily separable entity but one defined operationally based on the size of the material isolated and the methods used for its isolation. This heterogeneous material has a variety of sources, and its  $\text{DO}^{14}\text{C}$  signatures are complicated. However, these signatures have been able to provide remarkable insight into the processes governing the biogeochemical cycle of DOC.

Collection of bulk DOC for radiocarbon measurements requires properly cleaned equipment and the ability to store the sample in a manner that halts or minimizes postcollection alteration of the sample (e.g., microbial activity). Researchers use polar solvents and dilute acid to rinse the collection bottles. Seawater is filtered through precombusted quartz,

Vycor, or glass fiber filters with pore diameters of 0.7–1  $\mu\text{m}$  to remove POC, and the filtrate is stored in glass vessels.<sup>67</sup> Microbial activity is usually stopped by freezing the sample immediately after collection.<sup>67</sup>

Isolation and combustion of bulk DOC for radiocarbon analysis is complicated by the low concentration of DOC (approximately 40–100  $\mu\text{M}$ ) in the open ocean<sup>1</sup> relative to DIC (2000–2400  $\mu\text{mol/kg}$ )<sup>58</sup> and the presence of high concentrations of salt. DIC is removed by acidification of the seawater filtrate to a pH of approximately 3, typically with hydrochloric or phosphoric acid, to convert all dissolved inorganic carbon species to  $\text{CO}_2$ . It is recognized that this removes acid-volatile organic molecular species. Controversy

over the measurement of the concentration of DOC in seawater<sup>68</sup> resulted in the adoption of high-temperature combustion (HTC) techniques for oxidizing DOC to CO<sub>2</sub> for quantification. This technique is suited to concentration measurements, but the sample volumes used (200  $\mu$ L) do not provide enough material for a radiocarbon measurement. Methods developed for radiocarbon measurement must now demonstrate that they quantitatively oxidize the same amount of DOC to CO<sub>2</sub> as current HTC methods do (e.g., Druffel et al.<sup>69</sup>). Presently, oxidation of DOC is accomplished by UV oxidation, high-temperature wet combustion, or dry solid-phase combustion.

Armstrong et al.<sup>70</sup> first used UV oxidation to oxidize bulk DOC to CO<sub>2</sub>. To apply this method to radiocarbon analyses,<sup>71</sup> DIC was removed from a 100–200 L seawater sample by acidifying to pH 2 and bubbling with O<sub>2</sub>. The remaining carbon, defined as DOC, was oxidized by irradiation with a 1200 W mercury arc lamp, and the CO<sub>2</sub> evolved was trapped and prepared for radiocarbon analysis. In 1987, in a seminal paper, Williams and Druffel used the same oxidation method and reported on radiocarbon in DOC, demonstrating the parallel but offset nature of DO<sup>14</sup>C and DI<sup>14</sup>C profiles.<sup>6</sup> This study was further made possible because the advent of AMS allowed the analysis of samples as small as 5 L.<sup>6</sup> Subsequent improvements presently allow the analysis of 0.5–1 L of seawater for precise results on ocean samples. UV oxidation continues to be an important technique for the analysis of bulk DO<sup>14</sup>C samples<sup>7,72,73</sup> although it is expensive, time-consuming (1 day/sample), and not readily available to the community.

High-temperature combustions of wet samples<sup>74,75</sup> have been used in a few instances to oxidize DOC in seawater for radiocarbon analysis. Bauer et al.<sup>76</sup> compared HTC and UV oxidation methods for radiocarbon measurements on samples from the Atlantic and Pacific Oceans. Seawater samples (100 mL) were continuously injected in a stream of O<sub>2</sub> onto an oxidation catalyst at 900 °C, and the resulting CO<sub>2</sub> was collected on a molecular sieve.<sup>76</sup> The CO<sub>2</sub> was then converted to a graphite target for AMS analysis. Radiocarbon results from the HTC method were broadly consistent with those from the UV method but were less precise. The final error for individual measurements in  $\Delta^{14}\text{C}$  ranged from 3 to 6‰ and from 34 to 65‰ for UV oxidation and HTC, respectively.<sup>76</sup> The process blank for HTC was high compared to that for UV oxidation, 22 vs 2% of the total carbon collected, and was the main contributor to the high error. LeClercq et al.<sup>75</sup> used a supercritical oxidation system to oxidize DOC where acidified, purged seawater was saturated with O<sub>2</sub>, pressurized to 350 bar, and passed through a ceramic tube at 650 °C. This system also has a high blank, 0.1 mg C/L, and is not ideal for routine DO<sup>14</sup>C measurements.

Unfortunately, over the past decade, the community has not had access to a robust, relatively simple method for measuring marine DO<sup>14</sup>C. Many recent DOC studies instead report  $\Delta^{14}\text{C}$  values of particular DOC fractions. These DOC fractions have been isolated using a variety of different methods<sup>3,4,77,86,89,90</sup> that are detailed later in this review. The isolations can be based on size separations or chemical separations and are aimed at isolating specific individual compounds or compound classes. Isolation of defined fractions can facilitate analysis by concentrating the carbon in the desired fraction and allowing removal of the salt prior to combusting. Fraction-specific measurements also have the advantage of allowing a study of the biogeochemistry of

particular compounds with potentially well-defined sources, and they avoid some of the complexities generated by measuring  $\Delta^{14}\text{C}$  values for bulk DOC. The major drawback of these methods is that they only allow insight into what is often a small fraction (<20%) of the DOC reservoir.

## 4.2. Radiocarbon Measurements on Bulk DOC

Measurements of the radiocarbon content of marine DOC revolutionized our perception of the role of DOC in the marine carbon cycle. Certainly, DOC concentration measurements outlined the importance of DOC as a carbon reservoir, and the surface to deep ocean gradients in concentration hinted at a surface source for DOC. Early studies on bacterial degradation of DOC also suggested that at least some dissolved organic carbon was refractory over the time scale of incubations. But radiocarbon measurements were foremost in establishing the presence of a refractory DOC reservoir that exists well mixed throughout the water column to which a recent component is added in surface waters. Together with concentration measurements, these radiocarbon measurements suggested that, despite the large inventory of DOC (~650 Gt C), the flux of carbon through this reservoir was relatively small, on the order of ~0.1 Gt C/year, comparable in magnitude to the flux of DOC into the ocean from rivers and pore waters.<sup>5,78</sup>

Dissolved organic carbon of marine origin can be introduced into the meso- and bathypelagic ocean in three major ways. Up to 50% of the organic carbon fixed during marine primary production in the upper 250 m of the water column (euphotic zone) is thought to pass through the DOC reservoir.<sup>79</sup> A fraction of this carbon may escape bacterial degradation in surface waters and be subducted by various physical processes. Solubilization of POC sinking out of the euphotic zone can also release DOC into subsurface waters due to hydrolysis by particle-attached heterotrophic bacteria (e.g., Azam and Long<sup>80</sup>). Finally, significant gradients in DOC concentration between sediment pore waters and bottom waters, as well as near-bottom DOC concentration gradients, indicate that sediments may be a source of DOC to the subsurface ocean.<sup>81</sup> Other possible sources include hydrocarbon seeps and hydrothermal vents, but their contribution has not been adequately quantified. The radiocarbon content of DOC is perhaps the only property that is able to address the importance of each of these sources of DOC to the deep ocean and, even more critically, identify the residence time of DOC in the deep ocean. For example, DOC recently subducted from surface waters will have a  $\Delta^{14}\text{C}$  signature (DO<sup>14</sup>C) similar to that of DI<sup>14</sup>C at that same depth; DOC recently released from sinking particles will have DO<sup>14</sup>C values that are identical to that of sinking POC and, therefore, surface ocean DIC, but will be enriched in <sup>14</sup>C relative to DIC at the depth of sampling (in the subsurface ocean). The  $\Delta^{14}\text{C}$  of DOC released from sediments could span a broad range of values, but work by Bauer et al.<sup>74</sup> has shown that DOC released from sediments of the eastern North Pacific and the Santa Monica Basin is modern, i.e., enriched in bomb <sup>14</sup>C. While  $\Delta^{14}\text{C}$  can provide important DOC source information, perhaps the most important application of radiocarbon measurements in DOC studies has been to elucidate the range of its reactivity in riverine and marine environments.

The first DO<sup>14</sup>C measurements on subsurface samples were made by Williams et al.,<sup>71</sup> and nearly two decades later, the first DO<sup>14</sup>C depth profile was reported by Williams and

Druffel.<sup>6</sup> Together, these studies revealed several new features of the DOC cycle (see Figure 10). For example, the

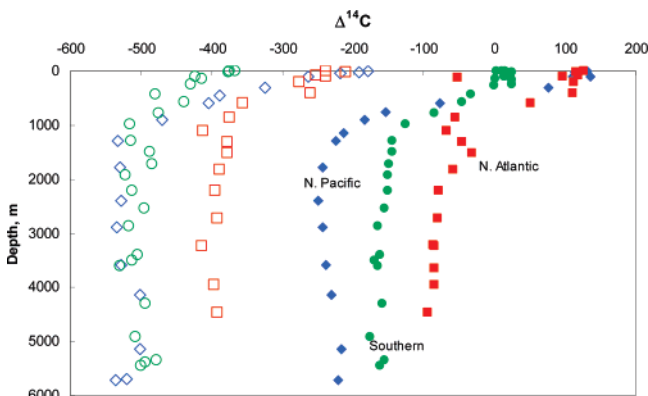


**Figure 10.** Depth profiles of  $\text{DO}^{14}\text{C}$  (open) and  $\text{DI}^{14}\text{C}$  (filled) in ‰, measured at three oceanic sites. North (N) Pacific ( $31^\circ\text{N}$ ,  $159^\circ\text{W}$ ; diamonds) and North (N) Atlantic ( $31^\circ\text{N}$ ,  $63^\circ\text{W}$ ; squares) data were taken from Druffel et al.<sup>5</sup> and correspond to their North Central Pacific and Sargasso Sea sites respectively. The data for the Southern Ocean site ( $54^\circ\text{S}$ ,  $176^\circ\text{W}$ ; circles) were taken from Druffel and Bauer.<sup>69</sup>

studies found DOC at every depth in the ocean is  $\sim 300\%$  depleted in  $^{14}\text{C}$  relative to DIC at that same depth. Also, vertical profiles of  $\text{DO}^{14}\text{C}$  and  $\text{DI}^{14}\text{C}$  values were shown to be similar in shape, which suggested that the distribution of both in the deep ocean is controlled by similar processes. Finally,  $\text{DO}^{14}\text{C}$  at 5700 m in the North Pacific was approximately  $-540\%$ .<sup>5,6</sup> If this average  $^{14}\text{C}$  age of approximately 6200 years for DOC represents its residence time in the ocean, then it exceeds the residence time of water in the deep ocean (1000–1500 radiocarbon years<sup>6</sup>). It was therefore anticipated that refractory (or  $^{14}\text{C}$ -depleted) DOC would be uniformly distributed with depth.<sup>6</sup> In addition, the penetration of bomb- $^{14}\text{C}$  in the DOC pool at depth,<sup>6</sup> as evidenced by the similarity in shape of  $\text{DO}^{14}\text{C}$  and  $\text{DI}^{14}\text{C}$  profiles within the top 1000 m of the water column, indicated that some mechanisms, such as advection or particle dissolution, must play a role in delivering modern DOC to the subsurface ocean.

There are currently several vertical profiles of  $\text{DO}^{14}\text{C}$  available in the literature for the North Pacific, but only one each for the North Atlantic and Southern Oceans.<sup>7,5,69,82,83</sup> The parallel profiles of  $\text{DI}^{14}\text{C}$  and  $\text{DO}^{14}\text{C}$  in the ocean (Figure 10) show a  $^{14}\text{C}$ -enrichment in both surface water reservoirs relative to deep waters. In the case of DIC, the surface enrichment represents a “re-setting” of the radiocarbon clock where DIC is free to exchange with  $^{14}\text{C}$ -rich atmospheric  $\text{CO}_2$ . The deep ocean depletion results from the decay of  $^{14}\text{C}$  during deep ocean circulation. The  $^{14}\text{C}$  depletion observed for DOC in the deep ocean can also be explained by the decay of radiocarbon during ocean circulation, but the surface  $^{14}\text{C}$  enrichment must be due to an entirely different mechanism—the addition of “new” or modern DOC during primary (autotrophic) production in surface waters—since direct exchange of the carbon atoms in DOC with atmospheric  $\text{CO}_2$  is not possible. However, despite the fact that the source carbon for autotrophic production of DOC in surface waters is DIC, the DOC reservoir in surface waters is depleted in  $^{14}\text{C}$  relative to DIC. The observed  $^{14}\text{C}$  depletion reflects the fact that surface ocean DOC is a mixture of both a recycled,  $^{14}\text{C}$ -depleted component that exists well mixed throughout the water column and a modern component added

during primary production. Surface ocean  $\text{DO}^{14}\text{C}$  can be accurately represented by an isotopic mass balance including an old DOC component upwelled from local deep waters and modern/excess DOC derived from photosynthesis, i.e.,

$$\text{DOC}_{\text{sfc}} = \text{DOC}_{\text{deep}} + \text{DOC}_{\text{xs}} \quad (7)$$

$$\Delta^{14}\text{C}_{\text{sfc}}\text{DOC}_{\text{sfc}} = \Delta^{14}\text{C}_{\text{deep}}\text{DOC}_{\text{deep}} + \Delta^{14}\text{C}_{\text{xs}}\text{DOC}_{\text{xs}} \quad (8)$$

where  $\Delta^{14}\text{C}_{\text{xs}} = \text{DI}^{14}\text{C}_{\text{sfc}}$  and the subscripts sfc, deep, and xs refer to surface, deep (3500–4000 m), and excess, respectively.

Solving the equations using data yields predicted  $\text{DO}^{14}\text{C}_{\text{sfc}}$  values that are identical, within measurement error, to measured values in the North Atlantic and North Pacific Oceans. For example, the measured  $\text{DO}^{14}\text{C}_{\text{sfc}}$  in the Sargasso Sea ( $31^\circ 50'\text{N}$ ,  $63^\circ 60'\text{W}$ ) is  $-210\%$ , not significantly different from the calculated value of  $-214\%$ .<sup>5</sup> A similar trend is obtained for the North Central Pacific ( $31^\circ\text{N}$ ,  $159^\circ\text{W}$ )—measured  $\text{DO}^{14}\text{C}_{\text{sfc}}$  is  $-153\%$  versus the calculated value of  $-155\%$ .<sup>6</sup> A similar calculation for the Southern Ocean ( $54^\circ\text{S}$ ,  $176^\circ\text{W}$ ) yields a predicted value of  $-398\%$  for  $\text{DO}^{14}\text{C}_{\text{sfc}}$  versus a measured value of  $-372\%$ . The more depleted value for  $\text{DO}^{14}\text{C}_{\text{sfc}}$  in the Southern Ocean is a result of the reduced value of  $\text{DI}^{14}\text{C}$  in surface waters at this location ( $\text{DI}^{14}\text{C}_{\text{sfc}} = 20\%$  in 1995/1996; Figure 10). In the Southern Ocean, the lower  $\text{DI}^{14}\text{C}$  results from greater vertical exchange between surface and subsurface waters, due to the weak thermocline, reducing the time available for surface waters to reach isotopic equilibrium.<sup>2</sup> The observed difference between the predicted and measured  $\text{DO}^{14}\text{C}_{\text{sfc}}$  values results from the difficulty in clearly decoupling the mass contributions of  $\text{DOC}_{\text{deep}}$  and  $\text{DOC}_{\text{xs}}$  in the Southern Ocean.

Mortazavi and Chanton<sup>98</sup> constructed a different mass balance in order to use Keeling plots to study  $\text{DO}^{14}\text{C}$  in the Pacific and Atlantic Oceans. Their analysis assumes that the entire vertical distribution of  $\text{DO}^{14}\text{C}$  can be explained as a mixture of two components, one modern and one refractory. In their presentation

$$\text{DOC}_z = \text{DOC}_{\text{ref}} + \text{DOC}_{\text{mod}} \quad (9)$$

$$\Delta^{14}\text{C}_z\text{DOC}_z = \Delta^{14}\text{C}_{\text{ref}}\text{DOC}_{\text{ref}} + \Delta^{14}\text{C}_{\text{mod}}\text{DOC}_{\text{mod}} \quad (10)$$

where the subscripts z, ref, and mod refer to depth, refractory, and modern.

Rearranging eqs 9 and 10 yields

$$\Delta^{14}\text{C}_z = \Delta^{14}\text{C}_{\text{mod}} + \frac{1}{\text{DOC}_z}[\text{DOC}_{\text{ref}}\Delta^{14}\text{C}_{\text{ref}} - \text{DOC}_{\text{ref}}\Delta^{14}\text{C}_{\text{mod}}] \quad (11)$$

In a Keeling plot, a graph of  $\Delta^{14}\text{C}_z$  versus  $1/\text{DOC}_z$  yields  $\Delta^{14}\text{C}_{\text{mod}}$  as the y-intercept when  $1/\text{DOC}_z$  approaches zero.<sup>63</sup> The slope of the line will consist of three parameters,  $\text{DOC}_{\text{ref}}$ ,  $\Delta^{14}\text{C}_{\text{ref}}$ , and  $\Delta^{14}\text{C}_{\text{mod}}$ . Thus,  $\Delta^{14}\text{C}_{\text{mod}}$  can be calculated without assuming a value for  $\Delta^{14}\text{C}_{\text{ref}}$ . An example of a Keeling plot for DOC in the North Pacific ( $31^\circ\text{N}$ ,  $159^\circ\text{W}$ ) is presented in Figure 11. The data are taken from Druffel et al.<sup>5</sup> and show a strong linear correlation ( $r^2 = 0.98$ ) between  $1/\text{DOC}_z$  and  $\Delta^{14}\text{C}_z$  at this site (similarly strong relationships are observed at other sites). The specific value of  $\Delta^{14}\text{C}_{\text{mod}}$  can be determined by applying a geometric mean regression

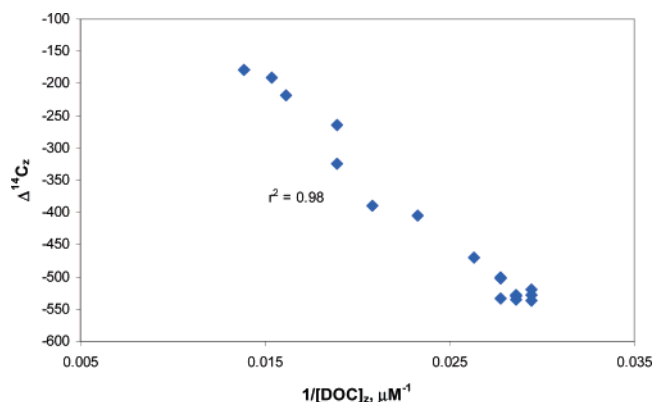


**Figure 11.** Linear relationship between  $1/[\text{DOC}]_z$  and  $\text{DO}^{14}\text{C}$  ( $\Delta^{14}\text{C}_z$ ) measured at a site in the North Central Pacific Ocean by Druffel et al.<sup>5</sup> after eq 11 in the text and according to Mortazavi and Chanton<sup>69</sup>

analysis of the data plotted as above and solving for  $\Delta^{14}\text{C}_z$  when the  $x$  variable ( $1/[\text{DOC}]_z$ ) is zero. For the North Pacific (Figure 11), this analysis yields a value of  $162 \pm 39\%$  ( $\pm$ standard error from the simple linear regression analysis) for  $\text{DO}^{14}\text{C}_{\text{mod}}$  ( $\Delta^{14}\text{C}_{\text{mod}}$ ).<sup>63</sup>

The most enriched  $\text{DI}^{14}\text{C}$  values in the North Pacific (June 1987) and North Atlantic (June 1989) at the time of sample collection were 135‰ and 127‰, respectively.<sup>5</sup> A recalculation of the Sargasso Sea (North Atlantic) data using the methods described by Mortazavi and Chanton<sup>69</sup> yields a Keeling intercept of  $135 \pm 26\%$ . This value, like the calculated  $\text{DO}^{14}\text{C}_{\text{mod}}$  for the North Pacific (above), is not statistically different from  $\text{DI}^{14}\text{C}$  in the same sample. The values calculated for  $\text{DO}^{14}\text{C}_{\text{mod}}$  at the Atlantic and Pacific sites are also in good agreement with  $\text{PO}^{14}\text{C}_{\text{susp}}$ . For example,  $\text{PO}^{14}\text{C}_{\text{susp}}$  had an average value of  $147 \pm 16\%$  in the upper 100 m at the North Pacific site, while  $\text{PO}^{14}\text{C}_{\text{susp}}$  at the North Atlantic site had a value of 138‰ at 20 m (the shallowest depth sampled).<sup>63</sup>

$\text{DO}^{14}\text{C}_{\text{mod}}$  calculated in the Southern Ocean ( $105 \pm 62\%$ ; December 1995/January 1996) was enriched in  $^{14}\text{C}$  relative to other carbon pools at the same location.<sup>53</sup> The highest  $\text{PO}^{14}\text{C}_{\text{susp}}$  measured was 32‰ at 16 m, and the highest  $\text{DI}^{14}\text{C}$  was 25‰. However, the large scatter in deep ocean DOC concentration measurements and the relatively small range in  $\text{DO}^{14}\text{C}$  values (between  $-366\%$  and  $-514\%$  here<sup>53</sup> versus between  $-210\%$  and  $-414\%$  in the North Atlantic,<sup>5</sup> for example) makes the  $\text{DO}^{14}\text{C}_{\text{mod}}$  determination from the Southern Ocean data set particularly sensitive to the fit of the regression. In general, the fact that the measured value of  $\text{PO}^{14}\text{C}_{\text{susp}}$  and the calculated value of  $\text{DO}^{14}\text{C}_{\text{mod}}$  in surface waters at each site contain bomb- $^{14}\text{C}$  shows that a significant fraction of each reservoir is replaced within a few years to decades.

The apparent, average age of DOC in the deep North Pacific is  $\sim 2000$  radiocarbon years older than DOC in the deep North Atlantic ( $-525 \pm 20\%$  versus  $-390 \pm 10\%$ ;<sup>5</sup> Figure 10). This age difference is the same order of magnitude as the  $\text{DI}^{14}\text{C}$ -derived water mass transit time between the deep North Atlantic and North Pacific of  $\sim 1400$  radiocarbon years (Figure 10). The similar magnitude of the Atlantic-to-Pacific radiocarbon age gradient obtained using both  $\text{DI}^{14}\text{C}$  and  $\text{DO}^{14}\text{C}$  has been interpreted to mean that most of the DOC in the deep ocean is advected, like DIC, from one ocean basin to another along the path of deep ocean circulation.<sup>5</sup> However,  $\text{DI}^{14}\text{C}$  values measured in deep waters

of the Southern Ocean ( $54^\circ\text{S}$ ,  $176^\circ\text{W}$ ) are intermediate between those of the North Atlantic and North Pacific sites (600–700 radiocarbon years between each basin), but  $\text{DO}^{14}\text{C}$  values imply a transit time of 1600 radiocarbon years between the North Atlantic and Southern Oceans and  $\sim 400$  years between the Southern Ocean and the North Pacific.<sup>2</sup> These discrepancies between  $\text{DI}^{14}\text{C}$ - and  $\text{DO}^{14}\text{C}$ -derived water mass transit times imply that, unlike the case for DIC, the addition of DOC to the various deep ocean basins may proceed by mechanisms other than simply passive transport of water masses. For example, the addition of dissolved compounds from sinking POC could provide an additional source of DOC to the subsurface ocean, while the preferential loss of relatively young DOC components during transport through the deep ocean could also lead to the observed discrepancy between ocean basins.

### 4.3. Radiocarbon Measurements on Chemically Fractionated DOC

The radiocarbon mass balance for  $\text{DOC}_{\text{xs}}$  described above assumes that only two radiocarbon end-members are present in surface waters. But what is the actual  $^{14}\text{C}$  distribution within DOC at various depths in the ocean? Although the discussion above has focused on the  $^{14}\text{C}$  content of total DOC, it is understood that this reservoir comprises a mixture of individual compounds, each with a distinct source and residence time in the ocean. One central question that arises from this model then is whether there is a continuum of  $^{14}\text{C}$  ages within DOC, or whether the average  $\text{DO}^{14}\text{C}$  value results from mixing varying concentrations of compounds with two or more distinct  $\Delta^{14}\text{C}$  signatures.<sup>2</sup> This question can only be answered if radiocarbon measurements are performed on specific DOC fractions and/or individual compounds.

The earliest marine DOC fractionation experiments for radiocarbon measurements were published in Druffel et al.<sup>5</sup> Here, radiocarbon measurements were made on DOC isolated by absorption onto chromatographic supports (XAD 2, 4, and 8) following acidification of seawater to approximately pH 3 with HCl. The mixture of compounds isolated by this solid-phase extraction (SPE) method was referred to as humic substances (containing primarily fulvic acids and some humic acids). In both the North Atlantic and North Pacific, DOC fractions isolated by this method were consistently depleted by as much as  $\sim 150\%$  in  $^{14}\text{C}$  relative to total DOC at each depth. These data showed conclusively that DOC at any given depth in the ocean consisted of a mixture of compounds with distinct  $\Delta^{14}\text{C}$  values. The  $^{14}\text{C}$  content of these isolates ranged from  $-329\%$  to  $-587\%$ , with the more  $^{14}\text{C}$ -depleted values observed in samples collected from deeper depths (e.g.,  $-358\%$  at 50 m versus  $-587\%$  at 3200 m in the Sargasso Sea; see Table 1). The observation that the  $^{14}\text{C}$ -age of humic substances ( $\sim 2500$  to 6000 years) was longer than the time required for one ocean mixing cycle implied that these compounds must exist throughout the water column as part of refractory DOC.

More recently, Benner et al.<sup>86</sup> reported  $\Delta^{14}\text{C}$  values for DOC extracted by SPE, using  $\text{C}_{18}$  as the chromatographic support, following acidification of the seawater (after Louchouart et al.<sup>87</sup>). All marine samples were located in the Arctic Ocean (latitudes  $> 70^\circ\text{N}$  and longitudes primarily between  $151^\circ\text{W}$  and  $166^\circ\text{W}$ ), and a variety of depths were sampled. The measured radiocarbon values are  $^{14}\text{C}$ -enriched (from  $\Delta^{14}\text{C} \sim -200\%$  in near-surface waters to  $-380\%$  at

**Table 1. Fraction-Specific Marine DO<sup>14</sup>C Data**

location	depth (m)	method	$\Delta^{14}\text{C}$ (‰)	ref
Sargasso Sea	50	XAD <sup>a</sup>	-329 to -402	5
	3200	XAD	-454 to -587	5
North Pacific	10	XAD	-342	5
Arctic Ocean (salinity > 30)	80	UF	-90	86
	3200	UF	-348	86
	11-50	C18 <sup>b</sup>	-199 to -262	86
	100-180	C18	-87 to -353	86
Mid Atlantic Bight (salinity > 35)	3000	C18	-378	86
	1-2	UF <sup>c</sup>	-89 to -182	90
	750-2600	UF	-376 to -403	90
	1-2	UF10 <sup>d</sup>	-6 to -8	90
North Atlantic Ocean	750-2600	UF10	-442 to -709	90
	3	UF	-5	4
	850	UF	-270	4
North Pacific Ocean	1500	UF	-262	4
	20	UF	-92	4
	900	UF	-381	4
Mid Atlantic Bight (marine)	1800	UF	-434	4
	2	UF	-10	8
	300	UF	-375	8
North Pacific Subtropical Gyre	750	UF	-255	8
	15	UF	10	3
	3	UF	46	3
	670	UF	-262 and -255	3

<sup>a</sup> XAD: macroporous polymeric beads that extract semipolar and nonpolar components of seawater. <sup>b</sup> C18: silica based resins that isolate hydrophobic DOC components. <sup>c</sup> UF: ultrafiltration using a 1000 Da (1 kDa) nominal molecular weight cutoff after prefiltering seawater through 0.1-0.2  $\mu\text{m}$  allows size fractionation of DOC. <sup>d</sup> UF10: same as UF but isolates molecules with molecular weights between 10,000 Da and 0.1/0.2  $\mu\text{m}$ .

3000 m; Table 1) relative to those reported for humic substances by Druffel et al.<sup>5</sup> Observed  $\Delta^{14}\text{C}$  differences between C18 and XAD isolates from all depths probably reflect either differences in source radiocarbon signatures (e.g., Benner et al.<sup>86</sup> identified a strong riverine contribution to Arctic Ocean samples) or resin-specific differences in the chemical composition of isolates.

#### 4.4. Radiocarbon Measurements on Size-Fractionated DOC

In recent years, several investigators have reported  $\Delta^{14}\text{C}$  values for size-fractionated DOC.<sup>4,8,77,86,88-91</sup> All of these studies focus on DOC isolated and concentrated by tangential flow ultrafiltration through a membrane of 1 nm pore-size, which is expected to retain compounds with molecular weights >1000 Da (>1 kDa; nominal molecular weight cutoff). Membrane filter type, precleaning procedures, and filtration time all have an impact on the quantity and the molecular characteristics of the DOC isolated.<sup>84</sup> To ensure reproducible and comparable results, Guo et al.<sup>92</sup> recommended strict protocols that include thorough precleaning of cartridges and monitoring of the DOC mass balance.

In open ocean environments, ultrafiltration using a 1 kDa nominal molecular weight cutoff will isolate 20-35% of the total DOC.<sup>127</sup> Radiocarbon measurements demonstrate that this high molecular weight (HMW) DOC is consistently enriched relative to total DOC at the same depth. However, with the exception of Aluwihare et al.<sup>8</sup> and Loh et al.,<sup>91</sup> no other study reports both DO<sup>14</sup>C and HMW DO<sup>14</sup>C values from the same location; in other studies, comparisons are made using published DO<sup>14</sup>C data from nearby locations. Aluwihare et al.<sup>8</sup> reported HMW DO<sup>14</sup>C and DO<sup>14</sup>C values for three depths (surface, 300 m, and 750 m) in the Mid-

Atlantic Bight (MAB; DO<sup>14</sup>C data provided by J. E. Bauer) and found that, at every depth, HMW DO<sup>14</sup>C was enriched relative to DO<sup>14</sup>C (-10‰ versus -32‰, -375‰ versus -414‰, and -255‰ versus -405‰, respectively). Guo et al.<sup>90</sup> concluded that there was a size-age relationship among various organic matter fractions in surface waters. Suspended POM represented the most modern end-member due to its production from recent photosynthesis, followed by HMW DOC/colloids in the size range >10 kDa to 0.2  $\mu\text{m}$  (average  $\Delta^{14}\text{C}$  = -45‰; range provided in Table 1), and DOC/colloids in the 1-10 kDa size range (average  $\Delta^{14}\text{C}$  = -144‰; range provided in Table 1). The oldest size fraction was identified as low molecular weight (LMW) DOC with molecular weights <1 kDa (average  $\Delta^{14}\text{C}$  = -240‰). This latter value was calculated by difference using an average bulk DO<sup>14</sup>C value of -200‰ for surface waters of the MAB (J. E. Bauer et al., unpublished) and measured  $\Delta^{14}\text{C}$  values for the various HMW fractions (above). Loh et al.<sup>4</sup> used mass balance calculations to reach a similar conclusion: that at all depths LMW DOC was more depleted in <sup>14</sup>C relative to HMW DOC. They reported HMW DO<sup>14</sup>C values of -5‰ and -92‰ for their North Atlantic and North Pacific sites, respectively. LMW DO<sup>14</sup>C at these same sites was -280‰ and -210‰, respectively. These data are consistent with the interpretation that HMW DOC is enriched in a component that is modern relative to total DOC and, by mass balance, LMW DOC. However, at most sites, HMW DOC is still significantly depleted in <sup>14</sup>C relative to surface water DIC. Finally, the size-age relationship identified by Guo et al.<sup>90</sup> is likely not a simple one, and all DOC fractions, including HMW and LMW DOC, probably consist of a mixture of compounds spanning a large  $\Delta^{14}\text{C}$  range. For example, Guo and Santschi<sup>93</sup> report data from estuarine and oceanic environments near Chesapeake Bay and Galveston Bay where the >1 kDa fraction is consistently enriched in <sup>14</sup>C relative to the >10 kDa fraction of DOC. The radiocarbon content and chemical composition of each individual DOC component primarily reflect its source and history, and the observed relationship to size is likely coincidental.

Surface HMW DO<sup>14</sup>C also shows marked variability (Table 1), suggesting that this fraction contains dynamic components with short residence times that are affected by local biological, chemical, and/or physical processes. This suggestion is consistent with some of the molecular-level analyses described below. For example, higher accumulations of recently produced, i.e., <sup>14</sup>C-enriched, HMW DOC may be found in areas of the ocean that are vertically stratified (e.g., HMW DO<sup>14</sup>C isolated from the North Pacific Subtropical Gyre had a DO<sup>14</sup>C value of +46‰; DI<sup>14</sup>C = 89  $\pm$  7‰; see Table 1), while surface waters that experience greater vertical mixing (e.g., eastern North Pacific Ocean) exhibit more depleted HMW DO<sup>14</sup>C signatures (-85  $\pm$  4‰ for the central California Current region; Aluwihare, unpublished). Similar physical controls were invoked to explain the observed variability in DO<sup>14</sup>C along a transect across the continental margin of the eastern North Pacific.<sup>121</sup> Alternatively, variations in the magnitude and type of HMW DOC sources (e.g., riverine versus marine) may also contribute to observed site-specific variations in HMW DO<sup>14</sup>C, both directly (e.g., by supplying components with unique  $\Delta^{14}\text{C}$  signatures) and indirectly (e.g., by supplying components that have long residence times in marine environments).

**Table 2.  $\Delta^{14}\text{C}$  Data for Compound Classes and Specific Compounds Isolated from HMW DOC**

location	depth (m)	method/class	$\Delta^{14}\text{C}$ (‰) <sup>a</sup>	ref
Mid Atlantic Bight	1–2	ethanol precipitation/carbohydrate-like	26/–112	77
North Atlantic	2	hydrolysis + ion exchange/carbohydrate-like <sup>b</sup>	13/–5	4
	2	hydrolysis + ion exchange/protein-like <sup>b</sup>	2/–5	
	2	solvent extraction/lipid <sup>b</sup>	–637–5	
	850	hydrolysis + ion exchange/carbohydrate-like <sup>b</sup>	–228/–270	4
	850	hydrolysis + ion exchange/protein-like <sup>b</sup>	–190/–270	
	850	solvent extraction/lipid <sup>b</sup>	–730/–270	
	1500	hydrolysis + ion exchange/carbohydrate-like <sup>b</sup>	–309/–262	4
	1500	hydrolysis + ion exchange/protein-like <sup>b</sup>	–215/–262	
Mid Atlantic Bight	1500	solvent extraction/lipid <sup>b</sup>	–830/–262	
	1–2	acid hydrolysis + HPLC/monosaccharides	49 to 92/–10	8
	300	acid hydrolysis + HPLC/monosaccharides	–120/–375	
North Pacific	750	acid hydrolysis + HPLC/monosaccharides	–59/–255	
	20	hydrolysis + ion exchange/carbohydrate-like	7/–92	4
North Pacific	20	hydrolysis + ion exchange/protein-like	–21/–92	
	20	solvent extraction/lipid	–551/–92	
	900	hydrolysis + ion exchange/carbohydrate-like	–302/–381	4
	900	hydrolysis + ion exchange/protein-like	–279/–381	
	900	solvent extraction/lipid	–864/–381	
	1800	hydrolysis + ion exchange/carbohydrate-like	–406/–434	4
	1800	hydrolysis + ion exchange/protein-like	–332/–434	
	1800	solvent extraction/lipid	–881/–434	
North Pacific	15	acid hydrolysis + HPLC/monosaccharides	57 ± 6/10	3
Subtropical Gyre	3	acid hydrolysis + HPLC/monosaccharides	89 ± 13/46	
	670	acid hydrolysis + HPLC/monosaccharides	–123 ± 10/–255	

<sup>a</sup>  $\Delta^{14}\text{C}$  is provided for the compound/compound class and total HMW DOC from the same sample (shown as compound  $^{14}\text{C}/\text{HMW DO}^{14}\text{C}$ ).

<sup>b</sup> HMW DOC samples (UF in Table 1) were extracted with dichloromethane/methanol to isolate the lipid fraction. The remaining aqueous fraction was either hydrolyzed using 6 N HCl, loaded onto a cation exchange column, and eluted with 1.5 N ammonium hydroxide to yield a protein-like fraction or hydrolyzed with 72% sulfuric acid, neutralized, and eluted from a cation/anion exchange mixed column with water to yield the carbohydrate-like fraction.

#### 4.5. Radiocarbon Measurements on Compounds and Compound Classes

Compound-specific radiocarbon measurements are necessary to fully resolve the nature of the  $^{14}\text{C}$  distribution in DOC. Within HMW DOC, the focus has been on the  $\Delta^{14}\text{C}$  signature of carbohydrates because of their high relative abundance within this DOC fraction (Table 2).<sup>8,94</sup> Early work on compound-class-specific  $\Delta^{14}\text{C}$  used the ethanol precipitation of carbohydrates and their chemically related compounds from HWM DOC to show that carbohydrate  $\Delta^{14}\text{C}$  values were enriched by up to 140‰ in surface waters (26‰ for carbohydrates versus –112‰ for HMW DOC; Table 2).<sup>77</sup> More recently, Loh et al.<sup>4</sup> used a combination of ion-exchange chromatography and acid hydrolysis to isolate a carbohydrate-like fraction from surface waters. Observed  $\Delta^{14}\text{C}$  values for this fraction (–7 to –13‰) were up to 100‰ enriched in  $\Delta^{14}\text{C}$  relative to HMW DOC (Table 2). Studies have also isolated carbohydrate components as identifiable monosaccharides from HMW DOC by acid hydrolysis and high-pressure liquid chromatographic (HPLC) separation and purification (Table 2).<sup>3,8</sup> In the MAB, all samples contained monosaccharides that were significantly enriched in  $^{14}\text{C}$  relative to the bulk HMW DOC.<sup>8</sup> The individual monosaccharides rhamnose, fucose, and xylose had  $\Delta^{14}\text{C}$  values between 49‰ and 92‰ in surface water compared to  $\text{DI}^{14}\text{C}$ ,  $\text{DO}^{14}\text{C}$ , and  $\text{HMW DO}^{14}\text{C}$  values of 59‰, –32‰, –10‰, respectively. At 300 m, the total monosaccharide fraction isolated from HMW DOC had a  $\Delta^{14}\text{C}$  value of –120‰ compared to –375‰ for  $\text{HMW DO}^{14}\text{C}$ ; and at 750 m, total monosaccharides were ~200‰ enriched in  $^{14}\text{C}$  relative to HMW DOC (–59‰ versus –255‰). The individual monosaccharides glucose, galactose, mannose, xylose, rhamnose, fucose, and arabinose, in HMW DOC isolated from surface waters of the North Pacific Subtropical Gyre, had  $\Delta^{14}\text{C}$  values between 47‰ and 67‰

(average 57 ± 6‰) at one site and a  $\Delta^{14}\text{C}$  value of 89 ± 13‰ at another. These values were not significantly different from those for DIC ( $\text{DI}^{14}\text{C} = 72 \pm 7\%$  and  $89 \pm 7\%$ ) and were somewhat enriched relative to HMW DOC ( $\text{HMW DO}^{14}\text{C} = 10\%$  and 46%).<sup>3</sup> At 670 m in the same region, the average  $\Delta^{14}\text{C}$  value of galactose, glucose, xylose, and mannose was –123 ± 10‰, only slightly enriched in  $\Delta^{14}\text{C}$  compared to DIC at the same depth (–155 ± 7‰) but significantly enriched relative to HMW DOC (–255‰). Aluwihare et al.<sup>8</sup> and Repeta and Aluwihare<sup>3</sup> were the first to report compound-specific  $\Delta^{14}\text{C}$  values for marine dissolved compounds, and they used the similar  $\Delta^{14}\text{C}$  values for monosaccharides and DIC as evidence that carbohydrates in surface waters are derived from recent photosynthesis. These data provided conclusive evidence for the accumulation of DOC derived from recent photosynthesis in the surface ocean and corroborated the two-end-member mixing model proposed by Williams and Druffel.<sup>6</sup> Using a simple model to relate the temporal evolution of  $\text{DO}^{14}\text{C}$  to DOC residence time in surface waters, Repeta and Aluwihare<sup>3</sup> concluded that carbohydrates must have a surface ocean residence time of ≤3 years or between 20 and 25 years at their North Pacific Subtropical Gyre sites. The uncertainty in residence time arises due to the observed temporal variability in surface ocean  $\text{DI}^{14}\text{C}$  over the last 50 years; that is,  $\text{DI}^{14}\text{C}$  had the same value at two separate times. See Figure 5, for example.

Although subsurface  $\Delta^{14}\text{C}$  values for carbohydrates encompass a large range of values,<sup>3,8</sup> they are also always enriched in  $^{14}\text{C}$  relative to the corresponding HMW DOC. In some cases,  $\Delta^{14}\text{C}$  values measured on mesopelagic carbohydrates are similar to, or slightly enriched compared to,  $\text{DI}^{14}\text{C}$  (e.g. at 750 m in the Mid Atlantic Bight  $\text{DI}^{14}\text{C} = -33\%$  and at 670 m in the North Pacific Subtropical Gyre  $\text{DI}^{14}\text{C} = -155\%$ ) and 670 m in the North Pacific Subtropical

Gyre ( $\text{DI}^{14}\text{C} = -155 \pm 7\%$ ); Table 2). More data on carbohydrate-specific  $\Delta^{14}\text{C}$  values are clearly needed before any conclusions can be drawn regarding the cycling of these compounds in subsurface waters. However, instances where subsurface  $\Delta^{14}\text{C}$  values that are enriched relative to the corresponding  $\text{DI}^{14}\text{C}$  are measured on components of DOC require that this material be delivered to deep waters by mechanisms other than water mass advection (e.g., dissolution of rapidly sinking particles).

A few investigators have also examined the  $\Delta^{14}\text{C}$  values of other compound classes isolated from HMW DOC (Table 2). Loh et al.<sup>4</sup> isolated a protein-like fraction which was enriched in  $\Delta^{14}\text{C}$  relative to HMW DOC; values were 2‰ (vs  $-5\%$  for HMW DOC) and  $-21\%$  (versus  $-92\%$  for HWM DOC; 20 m) for the protein-like fraction in surface Atlantic and Pacific waters, respectively (Table 2). These values reflect the addition of bomb- $^{14}\text{C}$  to the protein reservoir as well. However, the isolation scheme used for protein-like compounds by these investigators likely isolates other compounds as well; and so, the true-protein fraction may be more enriched in  $^{14}\text{C}$  if, for example, a group of refractory compounds with similar ion-exchange interactions were coisolated with proteins. In fact, proteins isolated from surface water HMW DOC following trichloroacetic acid (TCA) precipitation (after Tanoue et al.<sup>95</sup>) had a  $\Delta^{14}\text{C}$  value of  $+80\%$  at a site in the North Atlantic Subtropical Gyre,<sup>96</sup> not significantly different from the  $\text{DI}^{14}\text{C}$  and  $\text{PO}^{14}\text{C}_{\text{susp}}$  values at a nearby site.<sup>118</sup> Loh et al.<sup>4</sup> also reported  $\Delta^{14}\text{C}$  values for their protein-like fraction isolated from subsurface waters. This fraction is consistently enriched in  $^{14}\text{C}$  relative to the HMW DOC at all depths, but it becomes more depleted with depth (Table 2).

Solvent extractable lipids have also been isolated from HMW DOC for  $\Delta^{14}\text{C}$  measurements. Loh et al.<sup>4</sup> found that, at all depths examined, lipids were depleted in  $\Delta^{14}\text{C}$  relative to both total DOC and HMW DOC. So far, lipids represent the most  $^{14}\text{C}$ -depleted compounds isolated from DOC at open ocean sites—measured  $\Delta^{14}\text{C}$  values ranged from  $-551\%$  to  $-881\%$  (Table 2).<sup>4</sup> At similar depths and similar sites,  $\text{DO}^{14}\text{C}$  values ranged from  $-191\%$  to  $-533\%$ . It is noted here that lipids were isolated from HMW DOC, not total DOC. By definition, HMW DOC contains compounds with molecular weights exceeding 1000 Da. Therefore, lipids coisolated during ultrafiltration probably do not represent the composition or cycling of HMW DOC unless they are unusually large. Methods employed for the lipid extraction<sup>4</sup> would not have isolated lipids attached to other compounds through ester or ether bonds. Solvent extraction of total DOC isolated from bottom waters overlying hydrocarbon seeps in the Gulf of Mexico<sup>97</sup> yielded hydrophobic compounds that were strongly  $^{14}\text{C}$ -depleted: measured values were between  $-882\%$  and  $-991\%$ . Therefore, unlike the cases of proteins and carbohydrates, which are relatively polar and abundant intracellular biochemicals, lipids in DOC appear to be refractory and could represent the refractory end member of the two-component radiocarbon mass balance described previously.

#### 4.6. Sources of DOC Based on Radiocarbon Measurements

The mass balance discussed in section 4.2 (eqs 7 and 8) models surface water  $\text{DO}^{14}\text{C}$  as two components: one with a  $\Delta^{14}\text{C}$  value similar to surface ocean DIC (referred to as  $\text{DOC}_{\text{xs}}$ ) and another refractory end-member with a depleted

$\Delta^{14}\text{C}$  value ( $\text{DOC}_{\text{deep}}$ ). By definition  $\text{DOC}_{\text{xs}}$  must be derived from recent primary or secondary biological production in open ocean surface waters, where the ultimate source of carbon is DIC. Up to 50% of the organic carbon produced during photosynthesis in surface waters, or  $\sim 25$  Gt C/year, is channeled through the DOC reservoir,<sup>79</sup> providing more than enough carbon to sustain a marine DOC reservoir with a steady-state flux of  $\sim 0.1$  Gt C/year (determined based on radiocarbon measurements and reservoir size<sup>6</sup>). Vertical profiles of DOC concentration also suggest that as much as 50% of the surface ocean DOC reservoir may be added during biological production. This conclusion is confirmed by the recent direct measurement of bomb- $^{14}\text{C}$  in DOC components, primarily carbohydrates, and some proteins.<sup>3,4,8,77</sup> These latter studies also show that the fraction of DOC with molecular weights  $> 1000$  Da (i.e., HMW DOC) is more enriched in a modern or recent component relative to the total DOC pool, again consistent with the modern  $\Delta^{14}\text{C}$  values measured on carbohydrates and proteins isolated from HMW DOC. The carbohydrates and proteins directly identified above, for which  $^{14}\text{C}$  data are available, constitute  $< 10\%$  of the total DOC pool. However, isotope mass balances (eqs 7 and 8)<sup>5</sup> require that modern components typically exceed 30% of total DOC in the surface ocean. Therefore, other biochemicals, including proteins and carbohydrates that escape detection by the methods employed above, must also bear the modern  $\text{DO}^{14}\text{C}$  signature conferred by primary and secondary production in the surface ocean.

Rivers can also transport modern DOC to the ocean. In fact, the global flux of riverine DOC ( $\sim 0.2$  Gt C/year<sup>78</sup>) is large enough to sustain the marine DOC reservoir. Based on near-shore gradients in  $\text{DO}^{14}\text{C}$  and DOC concentration measured by Bauer et al.,<sup>85</sup> Mortazavi and Chanton<sup>98</sup> used eq 11 and Keeling plots to conclude that seasonal export of terrigenous organic carbon represents an important source of modern DOC to coastal waters of the MAB. Calculated  $\Delta^{14}\text{C}$  values for riverine DOC added to the coastal ocean ranged from 95‰ to 220‰. During the spring, when river discharge is expected to be highest, the input of terrestrial DOC was most prominent. The strongly enriched  $\text{DO}^{14}\text{C}$  signatures for  $\text{DOC}_{\text{mod}}$  in coastal waters during high riverine flux are consistent with  $\text{DO}^{14}\text{C}$  values measured in a variety of rivers. Raymond and Bauer<sup>99</sup> presented a compilation of riverine  $\text{DO}^{14}\text{C}$  in their Table 1. Although a large range in  $\text{DO}^{14}\text{C}$  values is observed, DOC in several rivers contains bomb- $^{14}\text{C}$ . The York River (Virginia) for example, carried DOC with  $\Delta^{14}\text{C}$  values between 159‰ and 257‰ (Table 3) at the time of measurement. Benner et al.<sup>86</sup> reported  $\text{DO}^{14}\text{C}$  values between  $-6$  and  $+307\%$  for four Arctic Rivers (Table 3) and concluded that young terrestrial DOC was exported from these rivers to the Arctic Ocean. Mayorga et al.<sup>100</sup> reported postbomb  $\Delta^{14}\text{C}$  values for all but one HMW DOC sample isolated from Amazonian Rivers (average HMW  $\text{DO}^{14}\text{C} = 182 \pm 67\%$ ; Mayorga et al.<sup>100</sup> refer to this fraction as DOC, but it is isolated by ultrafiltration using a  $> 1000$  Da molecular weight cutoff and is operationally identical to HMW DOC described here).

Although Mayorga et al.<sup>100</sup> found that HMW DOC in Amazonian Rivers contained bomb- $^{14}\text{C}$ , HMW  $\text{DO}^{14}\text{C}$  was enriched relative to atmospheric  $\text{CO}_2$  at the time of sample collection (between 1991 and 2003). As the  $\Delta^{14}\text{C}$  of atmospheric  $\text{CO}_2$  and DIC has been declining in all environments since the mid-1970s (Figures 5), the Amazon data show that, despite being of modern origin, HMW DOC, if

**Table 3.  $\Delta^{14}\text{C}$  Data for DOC Fractions Isolated from Some Freshwater and Estuarine Environments (for a More Complete Compilation, See Raymond and Bauer<sup>99</sup> and Bauer<sup>2</sup>)**

river	fraction	$\Delta^{14}\text{C}$ (‰)	ref
York	DOC	159 to 257	99
Hudson	DOC	-158 to 31	99
Arctic Rivers	DOC	-6 to 307	86
Amazonian Rivers	HMW DOC	182 ± 67	100
Amazon (1991)	DOC	28 ± 6	99
Itapeua	DOC on XAD	283 ± 13	101
Rio Negro	DOC on XAD	264 ± 15	101
Obidos	DOC on XAD	265 ± 12	101
Rio Negro	fulvic acids	344 ± 20	101
Rio Negro	humic acids	141 ± 18	101
Susquehanna	DOC	-81	91
	HMW DOC	4-108	91
	HMW-lipids <sup>a</sup>	-575	91
	protein-like <sup>a</sup>	16	91
	carbohydrate-like <sup>a</sup>	-129 ± 54	91

<sup>a</sup> See text and footnote 2 in Table 2 for definitions of abbreviations and isolation methods.

land-derived, must be pre-aged in the terrestrial environment for several decades prior to entering the rivers. In these same riverine samples,  $\Delta^{14}\text{C}$  values for dissolved  $\text{CO}_2$  are depleted in  $^{14}\text{C}$  relative to HMW DOC, suggesting that HMW DOC in these rivers is not derived from recent riverine primary production.<sup>100</sup> Finally, the study used the relationship between  $\Delta^{14}\text{C}$  of  $\text{CO}_2$  dissolved in Amazonian Rivers and  $\Delta^{14}\text{C}$  of atmospheric  $\text{CO}_2$  to conclude that these rivers do indeed transport terrestrial organic matter of very recent (<1 year) origin but that this organic matter is rapidly respired to  $\text{CO}_2$  during transport transferring the contemporary isotope signature to the dissolved  $\text{CO}_2$  pool. In summary, Amazonian Rivers transport terrestrial HMW DOC that contains bomb- $^{14}\text{C}$ ; however, the HMW DOC that is ultimately available for export to the coastal environment appears to represent a fraction that is several decades old. Although young terrestrial HMW DOC enters these rivers, it is respired within the riverine system.

Raymond and Bauer<sup>99</sup> made a similar observation for total DOC in the York River.  $\text{DO}^{14}\text{C}$  values for this river were relatively enriched (159‰ to 257‰), suggesting export of modern terrestrial DOC. During a 60-day degradation experiment in the fall, the DOC concentrations decreased by 136  $\mu\text{M C}$ , and a measurable decrease in the  $\text{DO}^{14}\text{C}$  value was observed. The largest change in both concentration and  $\Delta^{14}\text{C}$  values was observed over a year-long incubation of a DOC sample isolated during the summer. Approximately 63% of the DOC in this sample was removed over the 1-year period, and  $\text{DO}^{14}\text{C}$  decreased from 160‰ to -65‰ over the course of the incubation. A two-component radiocarbon mass balance yielded a  $\Delta^{14}\text{C}$  value of ~200‰ for the degraded DOC, a value similar to that of springtime  $\text{DO}^{14}\text{C}$  in the river. In general, these authors observed a linear relationship between the loss of DOC during biodegradation and the decrease in  $\text{DO}^{14}\text{C}$ . However, during the spring, when river flow is expected to be highest, only slight changes in DOC concentration and  $\Delta^{14}\text{C}$  values were observed over a 60 day degradation experiment. This sample also had the highest  $\text{DO}^{14}\text{C}$  measured during the study (257 ± 7‰), suggesting that it was carrying a large terrestrial DOC contribution. The authors conclude that while some rivers do carry modern DOC, biodegradation of the fresh DOC could ultimately lead to the export of old DOC.

In fact, not all rivers carry DOC containing bomb- $^{14}\text{C}$ . For example, Raymond and Bauer<sup>99</sup> noted that, of the eight rivers

sampled, three (the Hudson, Suquehanna, and Rappahannock) had prebomb  $\text{DO}^{14}\text{C}$  values (-158 ± 7‰, -81‰, and -91‰, respectively). Also,  $\text{POC}_{\text{susp}}$  in these rivers was often depleted in  $^{14}\text{C}$  relative to DOC, and the authors speculated that the  $\Delta^{14}\text{C}$  signature of  $\text{POC}_{\text{susp}}$  is controlled by the type of soils within the drainage basin and the dominant mode of erosion. These same processes may control the large variability observed for riverine  $\text{DO}^{14}\text{C}$  as well. In Amazonian Rivers, HMW DOC represents between 40% and 60% of the total DOC. Total  $\text{DO}^{14}\text{C}$  in the Amazon River was 28 ± 6‰ in 1991,<sup>99</sup> significantly depleted in  $^{14}\text{C}$  relative to HMW DOC (182 ± 67‰) discussed above. An isotope mass balance using total  $\text{DO}^{14}\text{C}$  and HMW  $\text{DO}^{14}\text{C}$  yields a  $\Delta^{14}\text{C}$  value between -70‰ and -200‰ for the remaining riverine LMW DOC, confirming the export of some old DOC by Amazon Rivers as well.

In an attempt to identify the composition of DOC along the Amazon River, Hedges et al.<sup>101</sup> recovered ~60% of the total DOC using XAD.  $\Delta^{14}\text{C}$  values for these isolated humic substances (humic and fulvic acids) in 1983 were 283 ± 13‰, 264 ± 15‰, and 265 ± 12‰ at Itapeua, Rio Negro, and Obidos, respectively (Table 3). In all cases, these values were enriched relative to atmospheric  $\text{CO}_2$  at the time (234 ± 3‰), suggesting that humic substances were stored in terrestrial soils for some time before entering the rivers, consistent with the observations of Mayorga et al.<sup>100</sup> for HMW DOC. In fact, Hedges et al.<sup>101</sup> were able to determine that some fraction of humic substances isolated as above must have been synthesized between 1963 and 1979, when  $\Delta^{14}\text{C}$  of  $\text{CO}_2$  in the atmosphere exceeded 300‰ (Table 3). These fraction-specific data also confirm what was observed with  $\text{DO}^{14}\text{C}$  and HMW  $\text{DO}^{14}\text{C}$ : terrestrial DOC may be stored on land before entering rivers and, presumably, the coastal ocean, but many of these fractions are still enriched in bomb- $^{14}\text{C}$  at the time of riverine export. It is noted here that, unlike terrestrial humic substances, humic substances isolated via XAD from marine systems are depleted in  $^{14}\text{C}$  throughout the water column at every location (see Table 1).

To identify the  $\Delta^{14}\text{C}$  signature of various HMW DOC sources to coastal organic matter, Loh et al.<sup>91</sup> sampled HMW DOC at the mouth of the Chesapeake Bay (salinity ~ 22) and one of its freshwater end members, the Susquehanna River. This study employed the same methods described in Loh et al.<sup>4</sup> (i.e., the isolation of chemical fractions by acid hydrolysis followed by ion exchange chromatography). At both sites, the total lipid extract of HMW DOC, only detectable during high river flow, was significantly depleted in  $^{14}\text{C}$  (-487‰, -575‰). This fraction was shown to consist primarily of  $\text{C}_{16}$ ,  $\text{C}_{18}$  fatty acids and  $\text{C}_{27}$ ,  $\text{C}_{29}$  sterols. The protein-like fraction contained bomb- $^{14}\text{C}$  and had an average  $\Delta^{14}\text{C}$  value of 27 ± 12‰ at both sites. However, the carbohydrate-like fraction was  $^{14}\text{C}$  depleted at the freshwater site (-129 ± 54‰) but contained bomb- $^{14}\text{C}$  at the saline site (10 ± 10‰). The presence of modern carbohydrates at the saline site is consistent with other studies showing that marine carbohydrates in the MAB are derived from recent biological production in surface waters.<sup>8,77</sup> For example, carbohydrates purified from HMW DOC by Aluwihare et al.<sup>8</sup> at a nearby site (in August 1996) had an average  $\Delta^{14}\text{C}$  value of 71 ± 21‰, not significantly different from  $\text{DI}^{14}\text{C}$  (50‰), suggesting recent photosynthetic production. Given the recent biological origin of carbohydrates in marine systems,<sup>8,77</sup> the presence of  $^{14}\text{C}$ -depleted carbohydrates in rivers is unexpected. This finding is especially surprising



because studies have shown that HMW carbohydrate fractions of DOC are compositionally similar in both freshwater and marine environments<sup>128</sup> and are, therefore, expected to have a similar origin in both environments. Based on these compositional studies, Loh et al.<sup>91</sup> suggested that proteins and carbohydrates have a similar residence time in saline environments. In terrestrial/freshwater environments, however, these fractions appear to have distinct residence times or sources. Although the protein fraction had a nearly identical  $\Delta^{14}\text{C}$  signature in both environments, its  $\delta^{13}\text{C}$  signature in each environment was distinct. As  $\delta^{13}\text{C}$  also carries source information, the authors concluded that proteins in each environment (saline versus freshwater) have distinct sources.<sup>91</sup> The similar  $\Delta^{14}\text{C}$  signature for proteins in both environments is compatible with this conclusion, as the current  $\Delta^{14}\text{C}$  values of  $\text{CO}_2$  in the atmosphere and surface ocean  $\text{DI}^{14}\text{C}$  are similar (Figure 5). In conclusion, the isotopic composition (both  $\delta^{13}\text{C}$  and  $\Delta^{14}\text{C}$ ) of proteins and carbohydrates in the bay implied that they were derived from *in-situ* production, but the isotopic composition of lipids suggested significant delivery of terrigenous/riverine lipids to the bay. While rivers transport both proteins and carbohydrates, the *in-situ* production of these compounds in the coastal environment appeared to overwhelm any terrestrial/riverine contribution.

The  $\text{DO}^{14}\text{C}$  values measured by Loh et al.<sup>91</sup> during both low and high flows were similar ( $-67 \pm 25\%$ ) at the bay and freshwater sites. During the high flow period, the HMW  $\text{DO}^{14}\text{C}$  value (108‰) at the freshwater site was more enriched in  $^{14}\text{C}$  relative to the low-flow period (4‰), likely reflecting a greater contribution from terrigenous HMW DOC during high flow. At the saline site, HMW  $\text{DO}^{14}\text{C}$  was similar during both low and high flow (41‰ versus 37‰), suggesting that *in-situ* production (autochthonous) in the bay and not riverine derived HMW DOC was more important for controlling HMW  $\text{DO}^{14}\text{C}$  values at the mouth of the Chesapeake Bay. This finding is consistent with the data from carbohydrates and proteins discussed above.

Aluwihare et al.<sup>8</sup> reported a value of  $-10\%$  for HMW  $\text{DO}^{14}\text{C}$  isolated from surface waters at a location near the Chesapeake Bay site of Loh et al.,<sup>91</sup> during August 1996 (1°E; higher salinity) (Table 1). The change in HMW  $\text{DO}^{14}\text{C}$  observed between 1996 and 2000 confirmed previous observations that a fraction of HMW DOC is dynamic and cycles on multiannual time scales. Whether the observed variability at this site results from changes in a photosynthetic contribution or a riverine contribution cannot be determined at this time.

Bauer and Druffel<sup>82</sup> observed a gradient in  $\text{DO}^{14}\text{C}$  values between coastal margin environments of both the western North Atlantic and North Central Pacific Oceans and their open ocean counterparts, the Sargasso Sea and North Central Pacific Ocean, respectively. Shown in Figure 12 are the DOC concentrations (Figure 12A) and  $\text{DO}^{14}\text{C}$  values (Figure 12B) for margin and open-ocean environments in the North Atlantic. At depths below 600 m in the North Atlantic, a positive gradient in DOC concentration between the margins and the open ocean was observed, suggesting that DOC may be available for export from the margin to open ocean sites. The  $\Delta^{14}\text{C}$  data at these same depths showed that  $\text{DO}^{14}\text{C}$  at the margin was depleted by as much as 75‰, relative to open ocean sites. Therefore, at depths below 600 m, margin DOC could represent a source of  $\Delta^{14}\text{C}$ -depleted organic matter to open ocean environments of the North Atlantic.

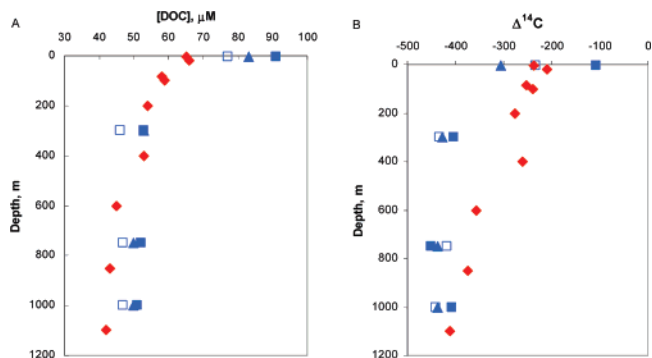


**Figure 12.** (A) Depth profiles of DOC concentration for three sites in the North Atlantic Ocean. Data for the northern (open squares), central (filled squares), and southern (filled triangles) western North Atlantic (WNA) margin sites were taken from Bauer et al.<sup>73</sup> Data for the Sargasso Sea site were obtained from Druffel et al.<sup>5</sup> (B) As above but for  $\text{DO}^{14}\text{C}$ .

Bauer and Druffel<sup>82</sup> used an isotopic mass balance for the Sargasso Sea to estimate the potential contribution from margin DOC to this open ocean site, and they concluded that between 96 and 99% of the DOC at the Sargasso Sea could be derived from margins. A similar calculation for the North Pacific Ocean (based on data from Druffel et al.<sup>5</sup> and Bauer et al.<sup>82</sup>) showed that 84–95% of DOC in the deep waters of an open ocean site in the central North Pacific could be derived from the eastern North Pacific continental margin. These values likely represent an overestimate because the authors assume only two sources of DOC to the deep open ocean: fresh DOC produced in surface waters at the open ocean site ( $\Delta^{14}\text{C} > 50\%$ , modern) and deep margin DOC ( $< -400\%$ ). Given that open ocean surface  $\text{DO}^{14}\text{C}$  is  $\sim -200\%$ , entrainment of this DOC in sinking water masses would deliver both fresh and refractory DOC components to the deep ocean. Second, deep waters of the open ocean are a mixture of several different water masses; for example, North Atlantic Deep Water and Antarctic Bottom Water represent sources of deep water to the Sargasso Sea. Therefore, other sources of DOC to deep waters of the Sargasso Sea, besides simply margin derived DOC, must be considered.

In summary, while DOC derived from recent photosynthesis must supply a significant fraction of modern carbon to surface waters of the open ocean, terrestrial DOC (both modern and aged) may be an important local source in some coastal environments. In addition, DOC derived from ocean margins may also be an important source of DOC to the meso- and bathypelagic open ocean. Although more work is necessary to establish the importance of each of these sources, it is likely that different riverine and margin systems are capable of exporting DOC with a broad range of  $\Delta^{14}\text{C}$  signatures to the marine environment.

## 4.7. Summary

We have attempted to provide the reader with a detailed introduction to the use of  $\Delta^{14}\text{C}$  in DOC cycling studies. As outlined in section 4.2,  $\Delta^{14}\text{C}$  measurements of bulk DOC have provided unique insight into the average residence time of DOC in the deep ocean ( $\sim 6000$  radiocarbon years) and potential modes of DOC distribution throughout the deep ocean. The presence of a well-mixed background DOC concentration throughout the water column coupled with observed deep ocean  $\text{DO}^{14}\text{C}$  gradients suggest that DOC is

passively transported along the path of deep ocean circulation. Alternatively, DOC mixing models suggest that recent/modern DOC is present throughout the deep ocean, requiring rapid delivery of DOC to some subsurface ocean environments. Furthermore, radiocarbon mass balances indicate the accumulation of significant amounts of fresh DOC derived from surface ocean biological production, and this is confirmed by compound-class- and compound-specific  $\Delta^{14}\text{C}$  measurements. These latter types of measurements also hint at the rapid input of DOC to subsurface waters.

Fraction-specific  $\Delta^{14}\text{C}$  measurements have confirmed that HMW DOC is significantly enriched in a modern component relative to total DOC in both surface and subsurface waters, and they further suggest that HMW DOC cycles on relatively short time scales. Carbohydrates in HMW DOC have been shown to represent a very dynamic DOC component in surface waters, with residence times of <3 years. The use of  $\Delta^{14}\text{C}$  to study sources of DOC to the ocean has shown that modern DOC can be added during both *in-situ* biological production and riverine delivery of terrigenous DOC. However, some riverine and margin systems may also be a source of relict DOC to open ocean environments.

It is clear from the preceding section that we still have only a limited understanding of the range of  $\Delta^{14}\text{C}$  values present within the total DOC reservoir, and so, we are unable to answer the question of whether  $\text{DO}^{14}\text{C}$  is comprised either of a continuum of  $\Delta^{14}\text{C}$  ages or of a few distinct age groups. We believe that identifying the range of DOC residence times within various marine environments must continue to be a research priority. This will be best achieved if the community embarks on time-series and compound-specific  $\Delta^{14}\text{C}$  measurements. In addition, a "routine"  $\text{DO}^{14}\text{C}$  measurement method must also be made available to the research community.

## 5. Particulate Organic Carbon

The seminal work of Williams and Druffel<sup>6</sup> demonstrating the parallel but offset radiocarbon profiles of DIC and DOC (Figure 9) led to speculation about the radiocarbon content of all pools of organic carbon in the marine environment. The low concentration of marine POC made it particularly challenging to study but especially intriguing. What insights into the nature and interactions of POC in the marine environment could be gained from studying its radiocarbon content? Would the smaller, perhaps more dynamic, POC pool be able to add insight to the old age observed in DOC? POC is a critical component of the marine carbon cycle, since it represents the major pathway to transport organic matter from the euphotic zone to the sediments. Within the water column, POC plays an important role in the microbial loop, sedimentation, biogeochemical cycling of a variety of elements, and particle dynamics.<sup>102</sup> This section will explore the information obtained from radiocarbon studies of both the suspended and sinking reservoirs of POC,  $\text{POC}_{\text{susp}}$ , and  $\text{POC}_{\text{sink}}$ , respectively.

Organic matter in the ocean exists as a continuum of sizes (Figure 9), and  $\text{POC}_{\text{susp}}$  is an operationally defined pool of carbon consisting of the material collected on a filter when seawater is passed through it.<sup>103</sup> By convention, 0.8  $\mu\text{m}$  is the filter cutoff used in oceanography, although some studies have been conducted with other filters (e.g., 1  $\mu\text{m}$  cutoff). This convention allows the collection of sufficient carbon for isotopic analysis but does limit the information that can be obtained with radiocarbon. Development of technologies

to isolate the discrete ranges of POC in sufficient quantity for radiocarbon analysis will improve the information that can be obtained from this isotope. Thorium isotope studies indicated that the suspended particulate pool has a residence time of 5–10 years,<sup>104</sup> and so,  $\text{POC}_{\text{susp}}$  was expected to have modern  $\Delta^{14}\text{C}$  values throughout the marine water column.  $\text{POC}_{\text{sink}}$  is the particulate organic material collected in sediment traps and generally consists of particles >50  $\mu\text{m}$  in size.<sup>105</sup> Transport of sinking material to the deep ocean occurs rapidly; for example, it takes approximately 1 month for foraminifera to travel from the surface to deep water in the North Atlantic.<sup>106</sup> Together, these observations suggest that, based on residence time alone,  $\Delta^{14}\text{C}$  of POC ( $\text{PO}^{14}\text{C}$ ), both sinking and suspended, will reflect modern surface-produced organic carbon at all depths in the ocean.

### 5.1. Collection/Isolation of POC

Collection of suspended POC for radiocarbon measurements is complicated by the low concentrations observed in the open ocean.  $\text{POC}_{\text{susp}}$  concentrations range from 0.04 to >30  $\mu\text{M C}$  in the open and coastal ocean with most open ocean concentrations <10  $\mu\text{M C}$  (Gardner et al.<sup>107</sup> and references therein). A notable exception is the Ross Sea in the Southern Ocean, which has  $\text{POC}_{\text{susp}}$  concentrations in the 100–200  $\mu\text{M C}$  range.<sup>69</sup> Currently, collection of enough material for a precise radiocarbon measurement, considering process blanks, requires the *in-situ* pumping of up to hundreds of liters of seawater through a filter; early studies required hundreds to thousands of liters.<sup>5</sup> Typically, prebaked quartz fiber filters with a nominal pore diameter of 0.8  $\mu\text{m}$  are used. Handling of filters introduces a higher process blank, and studies show that it represents from 1 to 15% of the carbon collected.<sup>82,108</sup>

$\text{POC}_{\text{sink}}$  is collected in sediment traps deployed over periods of time as long as 1 year. Material is collected in individual cups open to the flux of material for specified periods of time. Material collected at any point in time must remain in its individual cup as long as the trap remains deployed. Poisons are used to minimize or halt biological alteration of the material during this time; typically mercuric chloride, sodium azide, or formaldehyde is used. For carbon isotope studies, mercuric chloride is often preferred, since it does not contain carbon that may alter the isotopic content of  $\text{POC}_{\text{sink}}$ . Samples preserved with formalin have been analyzed,<sup>109,110</sup> and there appears to be no effect on the isotopes. Honda et al.<sup>110</sup> evaluated the effect of exposure to formalin on the  $\Delta^{14}\text{C}$  of sediment organic carbon (SOC). The  $\Delta^{14}\text{C}$  of SOC in sediments preserved for two weeks in formalin was not different from that of unpreserved SOC. Additionally, duplicate samples of  $\text{POC}_{\text{sink}}$  were allowed to remain in formalin for different periods of time and no significant changes in  $\text{PO}^{14}\text{C}_{\text{sink}}$  values were observed. The three pairs they measured had values of –46 and –55%, –6 and 1%, and 30 and 37%. These referred to preservation periods of 6.5 and 23.5, 4 and 21, and 1 and 18 months, respectively.

Prior to the isotope measurement, material collected on the filters or in sediment trap cups is acidified to remove inorganic carbon (i.e., carbonate) and the remaining POC is combusted to oxidize organic carbon to  $\text{CO}_2$ .<sup>5,83,111</sup> Methods used to remove carbonate from solid-phase samples can vary considerably and continue to be the subject of much discussion in the literature (Verardo et al.<sup>111</sup> and included references). We will not discuss this issue here, but we

caution researchers to carefully examine the available techniques, document the methods used, and realize that techniques appropriate for CN analyzers may not be appropriate for the sample size required for radiocarbon analysis.

## 5.2. Radiocarbon Studies of POC

The initial study of radiocarbon in POC was performed using  $\beta$ -decay counting methods on sinking particles collected in a sediment trap in the eastern sub-Arctic Pacific Ocean.<sup>112</sup> Results indicated that  $\text{PO}^{14}\text{C}_{\text{sink}}$  was greater than  $\text{DI}^{14}\text{C}$  in the ocean and suggested that there was a significant input of modern terrestrial organic matter to the traps through lateral advection. The advent of AMS led quickly to increased numbers of studies of the sinking as well as the suspended particulate pool.

The first study of the suspended pool demonstrated that its radiocarbon profile at both an oligotrophic site and a moderately eutrophic coastal basin was very different from that of either  $\text{DI}^{14}\text{C}$  or  $\text{DO}^{14}\text{C}$ .<sup>108</sup> At a station in the North Central Pacific (NCP; Figure 13),  $\text{PO}^{14}\text{C}_{\text{susp}}$  values ranged

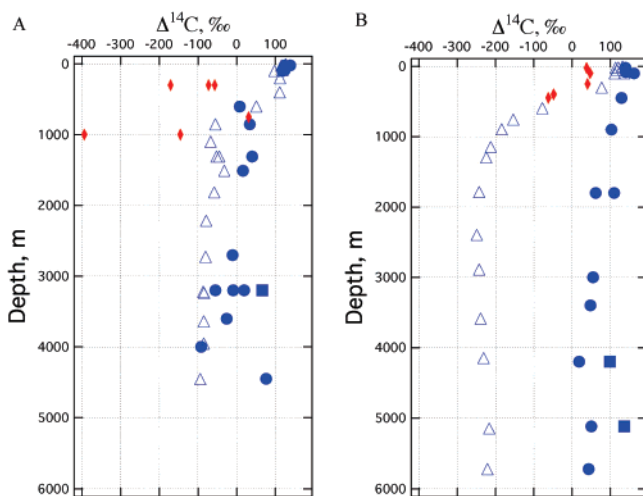


**Figure 13.** Radiocarbon profiles of  $\Delta^{14}\text{C}$  in DIC (open triangles),  $\text{POC}_{\text{susp}}$  (blue circles and red diamonds), and  $\text{POC}_{\text{sink}}$  (filled squares) in the (A) Atlantic and (B) Pacific Oceans.  $\text{PO}^{14}\text{C}_{\text{susp}}$  profiles are shown at open ocean sites (filled blue circles) and shallow margin sites (red diamonds). Data from Druffel et al.<sup>5,108</sup> and Bauer et al.<sup>73</sup>

from 139 to 43‰ from the surface to 5700 m, decreasing throughout the water column. In the Santa Monica Basin,  $\text{PO}^{14}\text{C}_{\text{susp}}$  showed similar values and trends with depth: from surface to 900 m,  $\text{PO}^{14}\text{C}_{\text{susp}}$  decreased from  $110 \pm 13\%$  at 100 and 200 m to approximately 0‰. These data confirmed that  $\text{POC}_{\text{susp}}$  has relatively short residence times (years to decades) in the ocean, even at depth, as bomb- $^{14}\text{C}$  was present in this reservoir throughout the water column.  $\text{PO}^{14}\text{C}_{\text{sink}}$  collected at approximately 4000 and 5000 m averaged 83‰ at the NCP site, greater than the  $\text{PO}^{14}\text{C}_{\text{susp}}$  at corresponding depths, indicating that the sinking pool has a higher percentage of material from the surface than the suspended pool; these data further suggested that distinct processes must act on sinking versus suspended POC in the deep ocean.

Figure 14 shows the processes that might be responsible for the decrease in  $\text{PO}^{14}\text{C}_{\text{susp}}$  with depth. The similarity of the surface water  $\text{PO}^{14}\text{C}_{\text{susp}}$  to the surface water  $\text{DI}^{14}\text{C}$  coupled with the presence of bomb carbon in  $\text{POC}_{\text{susp}}$  throughout the water column indicates that most of the POC

originates from recent primary production at the surface ocean. As only  $\text{POC}_{\text{sink}}$  can move through the water column rapidly enough to deliver bomb carbon to the deep ocean, measured  $\text{PO}^{14}\text{C}_{\text{susp}}$  requires that sinking particles disaggregate during their transit through the water column, supplying the suspended POC reservoir. However, the decrease in  $\text{PO}^{14}\text{C}_{\text{susp}}$  with depth was not expected based on concentration studies of POC and other studies of the residence time of POC in the water column. Druffel and Williams<sup>108</sup> speculated that older carbon was incorporated into the deeper  $\text{POC}_{\text{susp}}$  through either the sorption of old DOC from depth, chemo-synthetic production of  $\text{POC}_{\text{susp}}$  using older DIC from depth, or, for sites near margins or slopes, incorporation of older carbon from resuspended sediments. Additional sources not discussed in this study include the incorporation of  $^{14}\text{C}$ -dead material from hydrocarbon seeps and the possible effects of remineralization.  $\text{POC}_{\text{susp}}$  at the surface may be a mixture of a variety of types of organic matter,<sup>126</sup> each with its distinct radiocarbon content. Preferential remineralization of fresh/labile fractions could explain the decrease in  $\text{PO}^{14}\text{C}_{\text{susp}}$  with depth. Alternatively, the residence time (i.e., replacement time) of  $\text{POC}_{\text{susp}}$  may be longer at depth if, for example, the supply of carbon to this reservoir from  $\text{POC}_{\text{sink}}$  also decreases with depth. Although the values and depth trends were similar at both open ocean and basin sites, it seemed likely that different processes were responsible. In the basin, episodic resuspension of slope sediments was likely to add older sedimentary material to  $\text{POC}_{\text{susp}}$ . This process seemed far less likely at the north Pacific site. Assuming that sorption of DOC was the only process responsible for aging of  $\text{POC}_{\text{susp}}$  in the North Pacific, using the average  $\Delta^{14}\text{C}$  of  $\text{POC}_{\text{susp}}$  from samples below 1800 m and an average concentration of  $0.1 \mu\text{mol C/L}$ , mass balance calculations indicate that 14% of the carbon comes from DOC, or only 0.25% of the DOC pool. If sorption of DOC is a major source of the older carbon, then it is possible that  $\text{POC}_{\text{susp}}$  can transfer old carbon from mid-depths of the ocean to the deep water. Rau (1991)<sup>113</sup> pointed out that the uptake of deep water  $\text{DI}^{14}\text{C}$  onto POC by particle associated microorganisms could be another potential source for the decrease in  $\text{PO}^{14}\text{C}_{\text{susp}}$  with depth.

Further studies of radiocarbon in POC at the North Central Pacific (NCP) site coupled with a study in the Sargasso Sea (SS) in the Atlantic Ocean revealed similar patterns to those described above.<sup>5</sup>  $\text{PO}^{14}\text{C}_{\text{susp}}$  values were always similar to or greater than  $\text{DI}^{14}\text{C}$  values at corresponding depths, confirming the predominant origin from surface-produced organic matter. In the NCP,  $\text{PO}^{14}\text{C}_{\text{susp}}$  decreased from  $147 \pm 13\%$  in the surface 100 m to  $37 \pm 17\%$  between 4200 and 5720 m. The concentration of  $\text{POC}_{\text{susp}}$  decreased from 2.6 to  $0.05 \mu\text{M}$  over the same depth intervals.  $\text{PO}^{14}\text{C}_{\text{sink}}$  values collected at 4200 and 5120 m were 99 and 136‰, respectively, greater than  $\text{PO}^{14}\text{C}_{\text{susp}}$  at the same depths. In the Atlantic, the average value of  $\text{PO}^{14}\text{C}_{\text{susp}}$  in the surface 100 m was  $124 \pm 7\%$ , similar to that observed in the NCP, and the values at 3600, 4000, and 4450 m were -26, -92, and 76, respectively. The deep values showed far more variability than was observed in the NCP. The value for  $\text{PO}^{14}\text{C}_{\text{sink}}$  at 3200 m was 66‰, greater than that measured in the suspended pool at the same depths. The overall decrease in  $\Delta^{14}\text{C}$  values with increasing depth at both these sites was consistent with previous observations suggesting the incorporation of old carbon into  $\text{POC}_{\text{susp}}$  or the selective preservation of the older components of  $\text{POC}_{\text{susp}}$  as it cycles

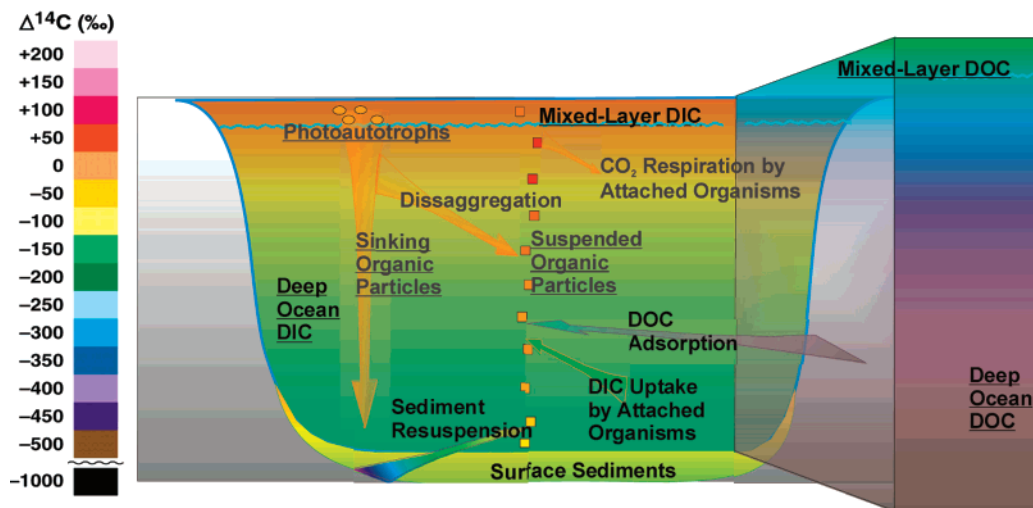


**Figure 14.** Processes potentially responsible for the decrease in  $\text{PO}^{14}\text{C}_{\text{susp}}$  with depth in the water column. Adapted with permission from Pearson, A., Biogeochemical Application of Compound-Specific Radiocarbon Analysis. Ph.D. Thesis, MIT/WHOI: 2000; 00-01. Copyright 2000 A. Pearson.

down the water column.  $\text{PO}^{14}\text{C}_{\text{sink}}$  was also greater than  $\text{PO}^{14}\text{C}_{\text{susp}}$  at similar depths. Decreasing concentrations of  $\text{POC}_{\text{susp}}$  with depth lend further support to the theory that part of the observed decrease in  $\text{PO}^{14}\text{C}_{\text{susp}}$  may result from a slower replacement time, from  $\text{POC}_{\text{sink}}$ , for this reservoir in the deep ocean.

The low concentration of POC and its likely rapid transport to depth imply that seasonal changes in  $\Delta^{14}\text{C}$  may be reflected in  $\text{POC}_{\text{susp}}$  at depth. To address the issue of seasonality,  $\text{PO}^{14}\text{C}$  measurements were made at four separate times at one site in the northeast Pacific Ocean (Station M): February, June, and October of 1992 and July of 1993.<sup>114</sup> This site showed seasonal variability in the magnitude of the POC flux with the highest pulses of  $10\text{--}25 \text{ mg C m}^{-2} \text{ day}^{-1}$  seen in the late spring and early fall and the lowest fluxes of  $1\text{--}3 \text{ mg C m}^{-2} \text{ day}^{-1}$  in the winter months.<sup>115</sup> Fluxes lower than normal were observed in spring 1992 due to the influence of an El Niño Southern Oscillation (ENSO) event.<sup>114</sup> At all times,  $\text{PO}^{14}\text{C}_{\text{susp}}$  decreased with depth although the magnitude and profile of the decrease varied from one sampling period to the next. The overall universal decrease suggested a similar mechanism governed by the observed drop in  $\Delta^{14}\text{C}$  with depth.<sup>114</sup> Values of  $\text{PO}^{14}\text{C}_{\text{susp}}$  measured in the surface 100 m averaged  $58 \pm 16$ ,  $65 \pm 7$ ,  $50 \pm 10$ , and  $75 \pm 7\text{‰}$  in February, June, October, and July, respectively. Compared to values from the deepest samples that were not influenced by resuspension of bottom sediments, gradients of 54, 105, 48, and 92‰ were observed in February, June, October, and July, respectively. Concentrations of POC decreased from values of  $3.29\text{--}6.53 \mu\text{M C}$  at the surface to  $0.1\text{--}0.2 \mu\text{M C}$  at depth. The most depleted profiles of  $\text{PO}^{14}\text{C}_{\text{susp}}$  were observed in June and July. The most similar radiocarbon profiles were observed in February 1992 and October 1992, the times with the greatest disparity in fluxes (October had the highest flux). In general, this study revealed that measurable changes in  $\text{PO}^{14}\text{C}_{\text{susp}}$  occur over relatively short time periods throughout the water column but that, despite the magnitude of the seasonal changes,  $\text{PO}^{14}\text{C}_{\text{susp}}$  always decreases with depth. If sorption of old DOC were the primary mechanism for the decrease, 7–12% of the  $\text{POC}_{\text{susp}}$  below the surface must be from this source.  $\text{PO}^{14}\text{C}_{\text{sink}}$  showed a negative correlation with flux; that is, the higher the  $\Delta^{14}\text{C}$ , the lower the flux of POC. This appeared counterintuitive given that the higher flux was presumed to

arise from surface-derived organic matter during periods of high primary productivity. However, the coincidence of the lowest concentrations of DOC with the highest particle fluxes and the lowest  $\text{PO}^{14}\text{C}_{\text{sink}}$  suggested that POC could strip DOC from the water column.<sup>82,114</sup> As this DOC has depleted  $\Delta^{14}\text{C}$  values, sorption of DOC would lead to a decrease in  $\text{PO}^{14}\text{C}_{\text{sink}}$  despite the higher flux of POC out of surface waters. This process also acts as a sink for DOC—transporting carbon from the DOC pool to the benthos.

Further studies of  $\text{PO}^{14}\text{C}_{\text{susp}}$  at Station M, the abyssal site in the northeast Pacific, confirmed the patterns noted above.<sup>116</sup> Surface values of  $\text{PO}^{14}\text{C}_{\text{susp}}$  were determined by the surface  $\text{DI}^{14}\text{C}$ ; thus, changes observed in surface values of  $\text{PO}^{14}\text{C}_{\text{susp}}$  at Station M over the course of almost a decade were related to the changes observed in  $\text{DI}^{14}\text{C}$  due to the decrease in atmospheric  $^{14}\text{C}$  content and the penetration of bomb  $^{14}\text{C}$  deeper into the water column (Figures 5 and 6). The importance of  $\text{DI}^{14}\text{C}$  in establishing the surface  $\text{PO}^{14}\text{C}_{\text{susp}}$  is demonstrated particularly well in the Southern Ocean, where surface values of both  $\text{DI}^{14}\text{C}$  and  $\text{PO}^{14}\text{C}_{\text{susp}}$  (approximately 3 to 25‰ and  $-20$  to  $-30\text{‰}$ , respectively) are much lower than those in the Pacific and Atlantic Oceans.<sup>69</sup> As demonstrated in Figures 6 and 10, the surface waters of the Southern Ocean have some of the most  $^{14}\text{C}$ -depleted DIC in the ocean, although the deep water values are in between those in the Atlantic and the Pacific. At Station M,  $\text{PO}^{14}\text{C}_{\text{susp}}$  values decreased by hundreds of per mille down the water column as the concentration of POC decreased by 2 orders of magnitude. A summary of the observations indicated that, at times of moderate flux,  $\text{PO}^{14}\text{C}_{\text{susp}}$  values in the deep water column were less than that at times of low flux. Anomalously high values of  $\Delta^{14}\text{C}$  at one time period appeared related to an anomalously high particle flux, different from what was seen during the seasonal study. It was suggested that, during this study, the flux of material was so great that the large amount of recently synthesized material passing through the water column contributed relatively larger amounts of modern carbon to the  $\text{POC}_{\text{susp}}$  pool and increased its  $\Delta^{14}\text{C}$  value. This conclusion is consistent with studies showing that the suspended particulate pool turns over rapidly in the water column.<sup>117</sup>

Bauer and Druffel<sup>82</sup> investigated the transport of organic material from the margins to ocean gyres as a potential source of older carbon to deep POC.  $\text{PO}^{14}\text{C}_{\text{susp}}$  at margin sites in

the western North Atlantic and eastern North Pacific Oceans was depleted relative to that measured in the central gyres of each ocean by greater than 100‰ in some cases. The carbon at these margin sites was more enriched in  $^{13}\text{C}$  than that expected from studies of carbon supplied to coastal waters, indicating that it had a primarily marine source. The source of this older, marine carbon was speculated to be resuspended shelf and slope sediments. Using the margin data in an isotopic mass balance to constrain the sources of carbon to  $\text{POC}_{\text{susp}}$  in the ocean gyres indicated that up to 85% of the gyre carbon may have been advected from the margins. Studies of  $\text{PO}^{14}\text{C}_{\text{sink}}$  support the transfer of older material from the margins. In the mid-Atlantic Bight,  $\text{PO}^{14}\text{C}_{\text{sink}}$  in a trap at 1000 m was 120‰ lower than that in a 30 m trap, suggesting the lateral transport of POC at depth to this site from margin environments.<sup>109</sup> In the Okinawa Trough in the western Pacific, values of  $\text{PO}^{14}\text{C}_{\text{sink}}$  less than surface  $\text{DI}^{14}\text{C}$  were attributed to lateral transport of material from the East China Sea.<sup>110</sup>

At this stage, of the potential explanations suggested for the observed decrease in  $\text{PO}^{14}\text{C}_{\text{susp}}$  with depth (Figure 14), sorption of old DOC seemed the most important with the advection of material from the shelf and slope temporally and spatially important. It is also clear that seasonal and secular events have a great influence on snapshot profiles in ways that are not always easy to predict and are more pronounced in POC than in DOC.

Temporal changes over time scales of 5 to 10 years are now evident in  $\text{DI}^{14}\text{C}$  in the open ocean. Reoccupation of central gyre sites in the Atlantic and Pacific Oceans (NCP and SS) allowed Druffel et al.<sup>118</sup> to study the link between significant changes in  $\text{PO}^{14}\text{C}_{\text{susp}}$  over a decade and the history of the bomb signal in the ocean. In the Pacific, there was a decrease of  $32 \pm 15\%$  in  $\text{PO}^{14}\text{C}_{\text{susp}}$  throughout the water column over a decade. In the Atlantic, there was a decrease of  $26 \pm 9\%$  in the upper 200 m and an increase of  $15 \pm 8\%$  between 600 and 3200 m over the same time period.<sup>118</sup> In the Pacific, it is likely that the change over time is due to the decrease in surface  $\text{DI}^{14}\text{C}$  observed as the bomb signal is reduced in the atmosphere. A box model relating the observed differences was used to estimate the overall turnover time for  $\text{POC}_{\text{susp}}$  to be 8.5 year. This value is consistent with early thorium isotope studies which indicated residence times between 5 and 10 years for the suspended particulate pool.<sup>104</sup> The heterogeneous changes in  $\Delta^{14}\text{C}$  seen at the deep Atlantic site made such calculations impossible and might be related to the episodic influence of lateral advection on  $\text{POC}_{\text{susp}}$ .

As more studies demonstrated the complexity of the influences on the radiocarbon content of POC, detailed studies of specific components of POC were undertaken. These studies focused on sinking POC because of sample size issues. Two samples of  $\text{POC}_{\text{sink}}$  collected at Station M in the Pacific Ocean in June 1993 were separated into four chemical groups.<sup>119,120</sup> The samples were collected at 3450 m and represented 9 day collections from the beginning and end of June. Organic matter was separated into total hydrolyzable amino acids (THAA), total carbohydrates (THCO), lipid, and acid-insoluble fractions.  $\text{POC}_{\text{sink}}$  was comprised of, on average, 26% THAA, 19% TCHO, 12.5% lipids, and 48% acid-insoluble material. Average radiocarbon values for the fractions were 56, 24, -1, and -23‰, respectively, and 15‰ for the bulk material. (A mass and their

radiocarbon values will not yield the bulk value because we are using average radiocarbon values that have not been mass adjusted.) The range of values observed in the different chemical fractions points to the complexity of the sources of  $\text{POC}_{\text{sink}}$  at depth and/or the mechanisms responsible for altering the biochemical composition of  $\text{POC}_{\text{sink}}$  as it passes through the water column. The values also confirm the influence of surface productivity on the entire pool of  $\text{POC}_{\text{sink}}$ .  $\text{DO}^{14}\text{C}$  values at this site varied between -244 and -312‰ in the surface 85 m from 1991 to 1993 and averaged -540‰ between 1600 and 4050 m,<sup>120,121</sup> and so, fraction-specific sorption of a small amount of DOC could drive the observed decrease in  $\Delta^{14}\text{C}$  of some chemical fractions. A more extensive study of the same compound classes isolated from  $\text{POC}_{\text{sink}}$  at the same depth and site showed the same general observations; that is, the lipids and an acid-insoluble fraction were depleted relative to the bulk  $\text{POC}_{\text{sink}}$ , and amino acids and carbohydrates had similar values.<sup>122</sup> Linear regressions of  $\Delta^{14}\text{C}_{\text{chemical group}}$  vs  $\text{PO}^{14}\text{C}_{\text{sink}}$  produced lines for each chemical group that intersected at the value of  $\text{DI}^{14}\text{C}$  at the surface. This suggests that at least a fraction of the carbon in each chemical group was acquired as a result of surface ocean biological production.

To test whether sorption of old DOC to POC could explain the decrease in  $\text{PO}^{14}\text{C}_{\text{sink}}$  with depth in the water column, Hwang et al.<sup>123</sup> incubated freshly collected, acidified, and dried plankton in freshly collected Sargasso Seawater for 13 days. In incubations with and without added poison,  $\text{PO}^{14}\text{C}$  values decreased over time, with the greatest changes observed in the experiments that contained no poison.  $\Delta^{14}\text{C}$  values decreased 96, 200, and 125‰ in the bulk, lipid, and acid-insoluble material in the unpoisoned experiment, respectively. Values decreased 30, 30, and 18‰ for the same classes in the poisoned experiment. Sorption of older DOC, enhanced by biological alteration of the surface of particles, was the most likely explanation for these results.

### 5.3. Summary

Studies of  $\text{PO}^{14}\text{C}$  have greatly enhanced our knowledge of the cycling of particulate matter in the ocean.  $\text{PO}^{14}\text{C}$  values throughout the water column, whether sinking or suspended, demonstrate that the primary source of this carbon is recent material produced at the surface of the ocean. As the surface ocean  $\text{DI}^{14}\text{C}$  has changed over the past decade, so has the  $\text{PO}^{14}\text{C}$ . Decreases in  $\text{PO}^{14}\text{C}$  values with increasing depth in the water column are universal: the global nature of these observations is summarized in Figure 15. In this figure, based on Druffel et al.,<sup>118</sup> we have plotted the difference between surface  $\text{DI}^{14}\text{C}$  ( $\text{DI}^{14}\text{C}_{\text{sfc}}$ ) and  $\text{PO}^{14}\text{C}_{\text{susp}}$  values observed at depth as a function of the distance of each sampling location to the nearest continental shelf as well as a function of the water column depth at each site. Here, we calculate  $\text{DI}^{14}\text{C}_{\text{sfc}}$  using the average of values measured in the surface 100 m and  $\text{PO}^{14}\text{C}_{\text{susp}}$  using the value measured approximately 500 m above bottom. The differences for all but one site (a value of -390‰ was calculated for one mid-Atlantic Bight site and is out of the range of the graphs in Figure 15) range between approximately 50 and 200‰ and are not related to the proximity to the continental shelf or to the water column depth. It is also evident from Figure 15 that more radiocarbon data are needed to understand the processes affecting  $\text{PO}^{14}\text{C}$ . Studies of  $\text{PO}^{14}\text{C}$  in a range of size fractions will provide more information about the sources and processes affecting this pool of carbon. The ability to measure smaller samples

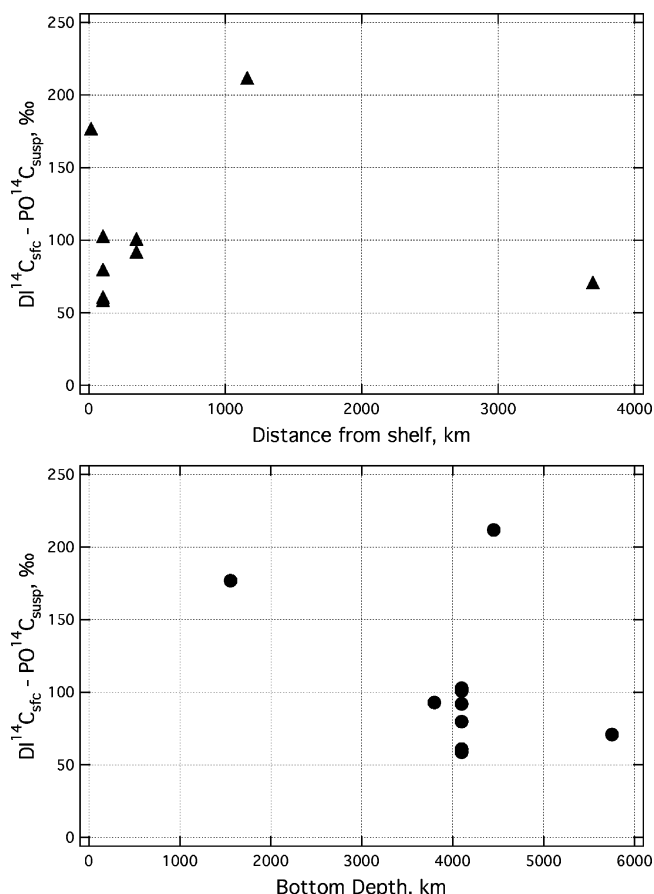


**Figure 15.** Difference between surface  $\text{DI}^{14}\text{C}$  and  $\text{PO}^{14}\text{C}_{\text{susp}}$  at depth as a function of distance from the nearest continental shelf and as a function of bottom depth.

accurately and precisely will make these types of studies easier. In general, however, coupled with evidence supporting both sorption of DOC and lateral advection of older material from the shelf and slope, the body of radiocarbon data discussed here suggests that both processes are equally important at all locations in the ocean.

Compound-specific radiocarbon analyses will also shed light on the nature and reactions of POC throughout the water column, although these studies are hindered by the ability to collect enough material for analysis. To date, only one study reports results on the radiocarbon content of specific compounds extracted from  $\text{POC}_{\text{susp}}$  in the mesopelagic ocean.<sup>35</sup> The study of archaeal lipids from the surface and 670 m in the subtropical North Pacific Gyre required the filtration of 100,000 and 200,000 L of seawater, respectively. Radiocarbon results on the individual archaeal lipids demonstrated that, at 670 m, the dominant metabolism of the archaea is autotrophy, yet some heterotrophy must be invoked to fully explain the observed  $\Delta^{14}\text{C}$  values. These data also demonstrate that the uptake of local DIC by particle associated microorganisms must be considered when interpreting the  $\text{PO}^{14}\text{C}_{\text{susp}}$  data. Studies targeting other biogeochemically relevant molecules will certainly lead to more insights into this dynamic pool of carbon although they will not be possible without the development of different methods for collection, isolation, and measurement.

## 6. Summary and Future Directions

The power of radiocarbon for studying the biogeochemistry of marine organic matter lies in its ability to provide

unique information about the sources and residence time of carbon in different reservoirs. Analytical advances in both isolation and measurement capabilities have allowed more detailed isotopic investigations of the carbon in the ocean's reservoirs and are expanding our understanding of ocean biogeochemistry. This review has focused on two reservoirs, DOC and POC, but the next decade will see a great expansion in the application of radiocarbon to biogeochemical studies. Compound-specific radiocarbon analyses will expand, and radiocarbon will be studied in process-specific chemicals in the water column, just as it is now in sediments. This will expand our knowledge of the pathways of carbon transfer in the modern ocean. For example, application to problems in microbial ecology, as has occurred with  $^{13}\text{C}$ , is likely to yield valuable and unique insights.

One poorly understood, but important, carbon reservoir in the ocean is that of black carbon (BC). BC has been recognized as an important link in the global carbon cycle for many years,<sup>124</sup> and it is a particular category of organic carbon in the ocean whose properties straddle the DOC/POC definition. Radiocarbon measurements of BC isolated in particles in the ocean will be critical for understanding the role of BC in the global carbon cycle. The supply of BC to the oceans from the atmosphere and the terrestrial environment is large enough to support the inventory found in the sediments, yet it is not known whether the BC that enters the ocean is transported rapidly to the underlying sediments or whether it is incorporated into pools of organic carbon that reside in the water column for significant periods of time prior to being removed to the sediments. The radiocarbon content of both the sources and the resident pool will help to answer this question.

The challenges for future researchers are many. As the capabilities of AMS and isolation techniques improve, the smaller samples that can be analyzed will require detailed and thorough assessments of process blanks and the implications of isotopic mixing and fractionation processes on  $^{14}\text{C}$  measurements.<sup>125</sup> The realization of continuous flow AMS for natural-level measurements, now under development, will open the field to new ways of using  $^{14}\text{C}$  to study biogeochemical processes. Completed research has demonstrated the power of radiocarbon, and the future holds promise for new and exciting applications.

## 7. Acknowledgments

We thank the National Science Foundation for support during the preparation of this manuscript. A.P.M. was supported by NSF Cooperative Agreement OCE-0228996; L.I.A. was supported by NSF CAREER OCE 05-48275. We thank Ann Pearson and an anonymous reviewer for helpful comments. John Hayes provided Figure 5, and Rick Healy put Figure 6 together. K. Brown and S. M. McNichol provided administrative support.

## 8. References

- (1) Hansell, D. A. In *Biogeochemistry of Marine Dissolved Organic Matter*; Hansell, D. A., Carlson, C. A., Eds.; Academic Press: New York, 2002.
- (2) Bauer, J. In *Biogeochemistry of Marine Dissolved Organic Matter*; Hansell, D. A., Carlson, C. A., Eds.; Academic Press: New York, 2002.
- (3) Repeta, D. J.; Aluwihare, L. I. *Limnol. Oceanogr.* **2006**, *51*, 1045.
- (4) Loh, A. N.; Bauer, J. E.; Druffel, E. R. M. *Nature* **2004**, *430*, 877.
- (5) Druffel, E. R. M.; Williams, P. M.; Bauer, J. E.; Ertel, J. R. J. *Geophys. Res., [Oceans]* **1992**, *97*, 15639.

- (6) Williams, P. M.; Druffel, E. R. M. *Nature* **1987**, *330*, 246.
- (7) Bauer, J. E.; Williams, P. M.; Druffel, E. R. M. *Nature* **1992**, *357*, 667.
- (8) Aluwihare, L. I.; Repeta, D. J.; Chen, R. F. *Deep-Sea Res., Part II=Top. Stud. Oceanogr.* **2002**, *49*, 4421.
- (9) Nagata, T.; Fukada, H.; Fukuda, R.; Koike, I. *Limnol. Oceanogr.* **2000**, *45*, 426.
- (10) Hansell, D. A.; Ducklow, H. W.; MacDonald, A. M.; Baringer, M. O. *Limnol. Oceanogr.* **2004**, *49*, 1084.
- (11) Libby, W. F. *Radiocarbon Dating*; 2nd ed.; University of Chicago Press: Chicago, 1955.
- (12) Godwin, H. *Nature* **1962**, *195*, 984.
- (13) Fairbanks, R. G.; Mortlock, R. A.; Chiu, T. C.; Cao, L.; Kaplan, A.; Guilderson, T. P.; Fairbanks, T. W.; Bloom, A. L.; Grootes, P. M.; Nadeau, M. J. *Quat. Sci. Rev.* **2005**, *24*, 1781.
- (14) Stuiver, M.; Polach, H. A. *Radiocarbon* **1977**, *19*, 355.
- (15) Donahue, D.; Linick, T. W.; Jull, A. J. T. *Radiocarbon* **1990**, *32*, 135.
- (16) Wigley, T. M. L. *Radiocarbon* **1981**, *23*, 173.
- (17) Currie, L. A. *J. Res. Natl. Inst. Stand. Technol.* **2004**, *109*, 185.
- (18) McNichol, A. P.; Jull, A. J. T.; Burr, G. S. *Radiocarbon* **2001**, *43*, 313.
- (19) Stuiver, M. *Radiocarbon* **1980**, *22*, 964.
- (20) Stuiver, M. *Radiocarbon* **1983**, *25*, 793.
- (21) Mook, W. G. *Radiocarbon* **1986**, *28*, 799.
- (22) Long, A. *Radiocarbon* **1995**, *37*, iii–iv.
- (23) Polach, H. A. In *Radiocarbon After Four Decades. An Interdisciplinary Perspective*; Taylor, R. E., Long, A., Kra, R., Eds.; Springer-Verlag: New York, 1992.
- (24) Tuniz, C.; Bird, J. R.; Fink, D.; Herzog, G. f. *Accelerator Mass Spectrometry: Ultrasensitive Analysis for Global Science*; CRC Press: Boca Raton, FL, 1998.
- (25) Turnbull, J. C.; Miller, J. B.; Lehman, S. J.; Tans, P. P.; Sparks, R. J.; Southon, J. *Geophys. Res. Lett.* **2006**, *33*, L01817.
- (26) Jull, A. J. T.; Burr, G. S. *Earth Planet. Sci. Lett.* **2006**, *243*, 305.
- (27) Ramsey, C. B.; Hedges, R. E. M. *Nucl. Instrum. Methods Phys. Res., Sect. B: Beam Interactions Mater. At.* **1994**, *92*, 100.
- (28) Ramsey, C. B.; Hedges, R. E. M. *Nucl. Instrum. Methods Phys. Res., Sect. B: Beam Interactions Mater. At.* **1997**, *123*, 539.
- (29) Santos, G. M.; Southon, J.; Griffin, S.; Beapre, S. R.; Druffel, E. R. M. *Nucl. Instrum. Methods Phys. Res., Sect. B: Beam Interactions Mater. At.*, in press.
- (30) Shah, S. R.; Pearson, A. Personal communication.
- (31) Roberts, M. L.; Schneider, R. J.; von Reden, K. F.; Wills, J. S. C.; Han, B. X.; Hayes, J. M.; Rosenheim, B. E.; Jenkins, W. J. *Nucl. Instrum. Methods Phys. Res., Sect. B: Beam Interactions Mater. At.*, in press.
- (32) Pearson, A.; McNichol, A.; Schneider, R. J.; von Reden, K. F. *Radiocarbon* **2000**, *40*, 61.
- (33) dos Santos, G. M.; Southon, J.; Griffin, S.; Beapre, S. R.; Druffel, E. R. M. *Nucl. Instrum. Methods Phys. Res., Sect. B: Beam Interactions Mater. At.*, in press.
- (34) Ingalls, A. E.; Anderson, R. F.; Pearson, A. *Mar. Chem.* **2004**, *92*, 91.
- (35) Ingalls, A. E.; Shah, S. R.; Hansman, R. L.; Aluwihare, L. I.; Santos, G. M.; Druffel, E. R. M.; Pearson, A. *Proc. Natl. Acad. Sci. U.S.A.* **2006**, *103*, 6442.
- (36) Currie, L. A.; Kessler, J. D.; Marolf, J. V.; McNichol, A.; Stuart, D. R.; Donoghue, J. C.; Donahue, D.; Burr, G. S.; Biddulph, D. *Nucl. Instrum. Methods Phys. Res., Sect. B: Beam Interactions Mater. At.* **2000**, *B172*, 440.
- (37) Vogel, J. S.; Nelson, D. E.; Southon, J. *Radiocarbon* **1987**, *29*, 323.
- (38) Hua, Q.; Zoppy, U.; Williams, A. A.; Smith, A. M. *Nucl. Instrum. Methods Phys. Res., Sect. B: Beam Interactions Mater. At.* **2004**, *B223–224*, 284.
- (39) Reimer, P. J.; Baillie, M. G. L.; Bard, E.; Bayliss, A.; Beck, J. W.; Bertrand, C. J. H.; Blackwell, P. G.; Buck, C. E.; Burr, G. S.; Cutler, K. B.; Damon, P. E.; Edwards, R. L.; Fairbanks, R. G.; Friedrich, M.; Guilderson, T. P.; Hogg, A. G.; Hughen, K. A.; Kromer, B.; McCormac, G.; Manning, S.; Ramsey, C. B.; Reimer, R. W.; Remmele, S.; Southon, J. R.; Stuiver, M.; Talamo, S.; Taylor, F. W.; van der Plicht, J.; Weyhenmeyer, C. E. *Radiocarbon* **2004**, *46*, 1029.
- (40) Reimer, P. *Radiocarbon: Int. J. Cosmogen. Isot. Res.* **2004**, *46*, 1029.
- (41) van der Plicht, J.; Beck, J. W.; Bard, E.; Baillie, M. G. L.; Blackwell, P. G.; Buck, C. E.; Friedrich, M.; Guilderson, T. P.; Hughen, K. A.; Kromer, B.; McCormac, F. G.; Ramsey, C. B.; Reimer, P. J.; Reimer, R. W.; Remmele, S.; Richards, D. A.; Southon, J. R.; Stuiver, M.; Weyhenmeyer, C. E. *Radiocarbon* **2004**, *46*, 1225.
- (42) Southon, J. *Radiocarbon* **2004**, *46*, 1239.
- (43) Levin, I.; Hesshaimer, V. *Radiocarbon* **2000**, *42*, 69.
- (44) Stuiver, M.; Quay, P. *Earth Planet. Sci. Lett.* **1981**, *53*, 349.
- (45) Meijer, H.; Vanderpligt, J.; Gislefoss, J. S.; Nydal, R. *Radiocarbon* **1995**, *37*, 39.
- (46) Levin, I.; Kromer, B. *Radiocarbon* **1997**, *39*, 205.
- (47) Levin, I.; Hesshaimer, V. *Radiocarbon* **2000**, *42*, 69.
- (48) Tans, P. P. In *SCOPE 16, Carbon Cycle Modelling*; Bolin, B., Ed.; Wiley, New York, 1981.
- (49) Nydal, R. In *Carbon-14 Measurements in Surface Water CO<sub>2</sub> from the Atlantic, Indian, and Pacific Oceans, 1965–1994*; Brenkert, A., Boden, T. A., Eds.; Carbon Dioxide Information Center, Oakridge National Laboratories; Oakridge, TN, 1998; ORNL-CDIAC 104.
- (50) Druffel, E. R. M. *Geophys. Res. Lett.* **1981**, *8*, 59.
- (51) Druffel, E. R. M. *J. Mar. Res.* **1987**, *45*, 667.
- (52) Stuiver, M.; Ostlund, G. *Radiocarbon* **1980**, *22*, 1.
- (53) Stuiver, M.; Ostlund, G. *Radiocarbon* **1983**, *25*, 1.
- (54) Ostlund, G.; Stuiver, M. *Radiocarbon* **1980**, *22*, 25.
- (55) Ostlund, G.; Grall, C. *Transient Tracers in the Ocean: North and Tropical Atlantic Tritium and Radiocarbon*. University of Miami, Rosenstiel School of Marine and Atmospheric Science, 1987.
- (56) Facility, O. D. *South Atlantic ventilaition experiment, chemical, physical an dCTD data report, legs 1–3*; Scripps Institution of Oceanography: 1992.
- (57) Facility, O. D. *South Atlantic ventilation experiment, chemical, physical and CTD data report, legs 4–5*; Scripps Institution of Oceanography: 1992.
- (58) Key, R. M.; Kozyr, A.; Sabine, C. L.; Lee, K.; Wanninkhof, R.; Bullister, J. L.; Feely, R. A.; Millero, F.; Mordy, C.; Peng, T.-H. *Global Biogeochem. Cycles* **2004**, *18*, GB4031.
- (59) Rubin, S.; Key, R. M. *Global Biogeochem. Cycles* **2002**, *16*, 1105.
- (60) Guilderson, T.; Schrag, D.; Kashgarian, M.; Southon, J. R. World Data Center A—Paleoclimatology Data Contribution Series #1999-043; NOAA/NGDC Paleoclimatology Program: Boulder, CO, 1999.
- (61) Guilderson, T. P.; Schrag, D. P.; Kashgarian, M.; Southon, J. J. *Geophys. Res., [Oceans]* **1998**, *103*, 24641.
- (62) Druffel, E. R. M. *Radiocarbon* **1996**, *38*, 563.
- (63) Grumet, N. S.; Abram, N. J.; Beck, J. W.; Dunbar, R. B.; Gagan, M. K.; Guilderson, T. P.; Hantoro, W. S.; Suwargadi, B. W. *J. Geophys. Res., [Oceans]* **2004**, *109*, CO5003.
- (64) Grumet, N. S.; Guilderson, T. P.; Dunbar, R. B. *J. Mar. Res.* **2002**, *60*, 725.
- (65) Grumet, N. S.; Guilderson, T. P.; Dunbar, R. B. *Radiocarbon* **2002**, *44*, 581.
- (66) Weidman, C. R.; Jones, G. A. *J. Geophys. Res., [Oceans]* **1993**, *98*, 14577.
- (67) Druffel, E. R. M.; Bauer, J. E.; Griffin, S. *Geochem. Geophys. Geosyst.* **2005**, *6*.
- (68) Hedges, J. I.; Lee, C. *Mar. Chem.* **1993**, *41*, 1.
- (69) Druffel, E. R. M.; Bauer, J. E. *Geophys. Res. Lett.* **2000**, *27*, 1495.
- (70) Armstrong, F. A. J.; Williams, P. M.; Strickland, J. D. H. *Nature* **1966**, *211*, 481.
- (71) Williams, P. M.; Oeschger, H.; Kinney, P. *Nature* **1969**, *224*, 256.
- (72) Druffel, E. R. M.; Williams, P. M.; Robertson, K.; Griffin, S.; Jull, A. J. T.; Donahue, D.; Toolin, L.; Linick, T. W. *Radiocarbon* **1989**, *31*, 523.
- (73) Bauer, J. E.; Druffel, E. R. M.; Wolgast, D. M.; Griffin, S. *Global Biogeochem. Cycles* **2001**, *15*, 615.
- (74) Bauer, J. E.; Reimers, C. E.; Druffel, E. R. M.; Williams, P. M. *Nature* **1995**, *373*, 686.
- (75) LeClercq, M.; VanderPlicht, J.; Meijer, H. A. J.; DeBaar, H. J. W. *Nucl. Instrum. Methods Phys. Res., Sect. B: Beam Interact. Mater. At.* **1997**, *123*, 443.
- (76) Bauer, J. E.; Williams, P. M.; Druffel, E. R. M. *Anal. Chem.* **1992**, *64*, 824.
- (77) Santschi, P. H.; Balnois, E.; Wilkinson, K. J.; Zhang, J. W.; Buffle, J.; Guo, L. D. *Limnol. Oceanogr.* **1998**, *43*, 896.
- (78) Hedges, J. I.; Oades, J. M. *Org. Geochem.* **1997**, *27* (7–8), 319.
- (79) Fuhrman, J. A.; Azam, F. *Mar. Biol.* **1982**, *66*, 109.
- (80) Azam, F.; Long, R. A. *Nature* **2001**, *414* (6863), 495.
- (81) Burdige, D. J.; Berelson, W. M.; Coale, K. H.; McManus, J.; Johnson, K. S. *Geochim. Cosmochim. Acta* **1999**, *63*, 1507.
- (82) Bauer, J. E.; Druffel, E. R. M. *Nature* **1998**, *392*, 482.
- (83) Bauer, J. E.; Druffel, E. R. M.; Williams, P. M.; Wolgast, D. M.; Griffin, S. *J. Geophys. Res., [Oceans]* **1998**, *103*, 2867.
- (84) Buesseler, K. O.; Bauer, J. E.; Chen, R. F.; et al. *Mar. Chem.* **1996**, *55*, 1.
- (85) Bauer, J. E.; Druffel, E. R. M.; Wolgast, D. M.; Griffin, S. *Deep-Sea Res., Part 2: Top. Stud. Oceanogr.* **2002**, *49* (20), 4387.
- (86) Benner, R.; Benitez-Nelson, B.; Kaiser, K.; Amon, R. M. W. *Geophys. Res. Lett.* **2004**, *31*, L05305.
- (87) Louchouart, P.; Opsahl, S.; Benner, R. *Anal. Chem.* **2000**, *72*, 2780.
- (88) Sannigrahi, P.; Ingall, E. D.; Benner, R. *Deep-Sea Res., Part I: Oceanogr. Res. Pap.* **2005**, *52*, 1429.

- (89) Santschi, P. H.; Guo, L. D.; Baskaran, M.; Trumbore, S.; Southon, J.; Bianchi, T. S.; Honeyman, B.; Cifuentes, L. *Geochim. Cosmochim. Acta* **1995**, *59*, 625.
- (90) Guo, L. D.; Santschi, P. H.; Cifuentes, L. A.; Trumbore, S. E.; Southon, J. *Limnol. Oceanogr.* **1996**, *41*, 1242.
- (91) Loh, A. N.; Bauer, J. E.; Canuel, E. A. *Limnol. Oceanogr.* **2006**, *51*, 1421.
- (92) Guo, L. D.; Santschi, P. M. *Mar. Chem.* **1996**, *55*, 133.
- (93) Guo, L. D.; Santschi, P. H. *Rev. Geophys.* **1997**, *35*, 17.
- (94) Benner, R.; Pakulski, J. D.; McCarthy, M.; Hedges, J. I.; Hatcher, P. G. *Science* **1992**, *255*, 1561.
- (95) Tanoue, E.; Nishiyama, S.; Kamo, M.; Tsugita, A. *Geochim. Cosmochim. Acta* **1995**, *59*, 2643.
- (96) Meador, T. B.; Aluwihare, L. I.; Mahaffey, C. *Limnol. Oceanogr.*, in press.
- (97) Wang, X. C.; Chen, R. F.; Whelan, J.; Eglinton, L. *Geophys. Res. Lett.* **2001**, *28*, 3313.
- (98) Mortazavi, B.; Chanton, J. P. *Limnol. Oceanogr.* **2004**, *49*, 102.
- (99) Raymond, P. A.; Bauer, J. E. *Org. Geochem.* **2001**, *32* (4), 469.
- (100) Mayorga, E.; Aufdenkampe, A. K.; Masiello, C. A.; Krusche, A. V.; Hedges, J. I.; Quay, P. D.; Richey, J. E.; Brown, T. A. *Nature* **2005**, *436*, 538.
- (101) Hedges, J. I.; Ertel, J. R.; Quay, P. D.; Grootes, P. M.; Richey, J. E.; Devol, A. H.; Farwell, G. W.; Schmidt, F. W.; Salati, E. *Science* **1986**, *231*, 1129.
- (102) Verdugo, P.; Alldredge, A. L.; Azam, F.; Kirchman, D. L.; Passow, U.; Santschi, P. H. *Mar. Chem.* **2004**, *92*, 67.
- (103) Hedges, J. I. In *Biogeochemistry of Marine Dissolved Organic Matter*; Hansell, D. A., Carlson, C. A., Eds.; Academic Press: New York, 2002.
- (104) Bacon, M. P.; Anderson, R. F. *J. Geophys. Res., [Oceans]* **1982**, *87*, 2045.
- (105) Lee, C.; Wakeham, S.; Arnosti, C. *Ambio* **2004**, *33*, 565.
- (106) Deuser, W. G. *Deep-Sea Res., Part I: Oceanogr. Res. Pap.* **1986**, *33*, 225.
- (107) Gardner, W. D.; Mishonov, A.; Richardson, M. J. *Deep-Sea Res., Part II: Top. Stud. Oceanogr.* **2006**, *53*, 718.
- (108) Druffel, E. R. M.; Williams, P. M. *Nature* **1990**, *347*, 172.
- (109) Anderson, R. F.; Rowe, G. T.; Kemp, P. F.; Trumbore, S.; Biscaye, P. E. *Deep-Sea Res., Part II: Top. Stud. Oceanogr.* **1994**, *41*, 669.
- (110) Honda, M. C.; Kusakabe, M.; Nakabayashi, S.; Katagiri, M. *Mar. Chem.* **2000**, *68*, 231.
- (111) Verardo, D. J.; Froelich, P. N.; McIntyre, A. *Deep-Sea Res., Part A: Oceanogr. Res. Pap.* **1990**, *37*, 157.
- (112) Druffel, E. R. M.; Honjo, S.; Griffin, S.; Wong, C. S. *Radiocarbon* **1986**, *28*, 397.
- (113) Rau, G. H. *Nature* **1991**, *350*, 116.
- (114) Druffel, E. R. M.; Bauer, J. E.; Williams, P. M.; Griffin, S.; Wolgast, D. J. *Geophys. Res. [Oceans]* **1996**, *101*, 20543.
- (115) Smith, K. L.; Kaufmann, R. S.; Baldwin, R. J. *Limnol. Oceanogr.* **1994**, *39*, 1101.
- (116) Druffel, E. R. M.; Griffin, S.; Bauer, J. E.; Wolgast, D. M.; Wang, X. C. *Deep-Sea Res., Part II: Top. Stud. Oceanogr.* **1998**, *45*, 667.
- (117) Sherrell, R. M.; Field, M. P.; Gao, Y. *Deep-Sea Res., Part II: Top. Stud. Oceanogr.* **1998**, *45*, 733.
- (118) Druffel, E. R. M.; Bauer, J. E.; Griffin, S.; Hwang, J. *Geophys. Res. Lett.* **2003**, *30*, 1744.
- (119) Wang, X. C.; Druffel, E. R. M.; Griffin, S.; Lee, C.; Kashgarian, M. *Geochim. Cosmochim. Acta* **1998**, *62*, 1365.
- (120) Wang, X. C.; Druffel, E. R. M.; Lee, C. *Geophys. Res. Lett.* **1996**, *23*, 3583.
- (121) Bauer, J. E.; Druffel, E. R. M.; Wolgast, D. M.; Griffin, S.; Masiello, C. A. *Deep-Sea Res., Part II: Top. Stud. Oceanogr.* **1998**, *45*, 689.
- (122) Hwang, J.; Druffel, E. R. M.; Komada, T. *Global Biogeochem. Cycles* **2005**, *19*, GB2018.
- (123) Hwang, J. S.; Druffel, E. R. M.; Bauer, J. E. *Mar. Chem.* **2006**, *98*, 315.
- (124) Goldberg, E. D. *Black Carbon in the Environment; Properties and Distribution*; John Wiley and Sons: New York, 1986.
- (125) Zencak, Z.; Reddy, C. M.; Teuten, E. L.; Xu, L.; Gustafsson, O. *Anal. Chem.*, in press.
- (126) Gelin, Y.; Prentice, K. M.; Baldock, J. A.; Hedges, J. I. *Environ. Sci. Technol.* **2001**, *35*, 3519.
- (127) Benner, R. In *Biogeochemistry of Marine Dissolved Organic Matter*; Hansell, D. A., Carlson, C. A., Eds.; Academic Press, New York, 2002.
- (128) Repeta, D. J.; Quan, T. M.; Aluwihare, L. I.; Accardi, A. M. *Geochim. Cosmochim. Acta* **2002**, *66*, 955.

CR050374G